Planetary transit candidates in the CoRoT LRa01 field[*]

L. Carone[1], D. Gandolfi[2,3], J. Cabrera[4,5], A. P. Hatzes[3], H. J. Deeg[6,7], Sz. Csizmadia[4], M. Pätzold[1], J. Weingrill[8], S. Aigrain[9], R. Alonso[10], A. Alapini[11], J.-M. Almenara[6,7,12], M. Auvergne[13], A. Baglin[13], P. Barge[12], A. S. Bonomo[12], P. Bordé[14], F. Bouchy[15,16], H. Bruntt[13], S. Carpano[2], W. D. Cochran[17], M. Deleuil[12], R. F. Díaz[15,16], S. Dreizler[18], R. Dvorak[19], J. Eislöffel[3], P. Eigmüller[3], M. Endl[17], A. Erikson[4], S. Ferraz-Mello[20], M. Fridlund[2], J.-C. Gazzano[12,21], N. Gibson[9,11], M. Gillon[10,22], P. Gondoin[2], S. Grziwa[1], E.W. Günther[3], T. Guillot[21], M. Hartmann[3], M. Havel[21], G. Hébrard[15], L. Jorda[12], P. Kabath[4,23], A. Léger[14], A. Llebaria[12], H. Lammer[8], C. Lovis[10], P. J. MacQueen[17], M. Mayor[10], T. Mazeh[24], C. Moutou[12], L. Nortmann[18], A. Ofir[24], M. Ollivier[14], H. Parviainen[6,7], F. Pepe[10], F. Pont[11], D. Queloz[10], M. Rabus[6,7,25], H. Rauer[4,26], C. Régulo[6,7], S. Renner[4,27,28], R. de la Reza[29], D. Rouan[13], A. Santerne[12], B. Samuel[14], J. Schneider[5], A. Shporer[24,30], B. Stecklum[3], L. Tal-Or[24], B. Tingley[6,7], S. Udry[10], and G. Wuchterl[3]

(Affiliations can be found after the references)

Received ...; accepted ...

ABSTRACT

Context. *CoRoT* is a pioneering space mission whose primary goals are stellar seismology and extrasolar planets search. Its surveys of large stellar fields generate numerous planetary candidates whose lightcurves have transit-like features. An extensive analytical and observational follow-up effort is undertaken to classify these candidates.

Aims. The list of planetary transit candidates from the *CoRoT* LRa01 star field in the Monoceros constellation towards the Galactic anti-center is presented. The *CoRoT* observations of LRa01 lasted from 24 October 2007 to 3 March 2008.

Methods. 7 470 chromatic and 3 938 monochromatic lightcurves were acquired and analysed. Instrumental noise and stellar variability were treated with several filtering tools by different teams from the *CoRoT* community. Different transit search algorithms were applied to the lightcurves.

Results. Fifty-one stars were classified as planetary transit candidates in LRa01. Thirty-seven (i.e., 73 % of all candidates) are "good" planetary candidates based on photometric analysis only. Thirty-two (i.e., 87 % of the "good" candidates) have been followed-up. At the time of this writing twenty-two cases have been solved and five planets have been discovered: three transiting hot-Jupiters (*CoRoT*-5b, *CoRoT*-12b, and *CoRoT*-21b), the first terrestrial transiting planet (*CoRoT*-7b), and another planet in the same system (*CoRoT*-7c, detected by radial velocity survey only). Evidences of another non-transiting planet in the *CoRoT*-7 system, namely *CoRoT*-7d, have been recently found.

Key words. techniques: photometric - techniques: radial velocities - techniques: spectroscopic - stars: planetary systems - binaries: eclipsing

1. Introduction

This paper summarizes the planetary candidates found in the LRa01 exoplanet star field and some preliminary scientific results from the combination of *CoRoT* photometry with ground based follow-up observations. The *CoRoT* IRa01 and LRc01 runs have already been reported by Carpano et al. (2009) and Moutou et al. (2009), and Cabrera et al. (2009), respectively.

The LRa01 run, from 24 October 2007 to 3 March 2008, was the second long pointing of *CoRoT* after the LRc01 field (Cabrera et al. 2009). The LRa01 star field contains 11 408 pre-selected stars covering a sky-area within the coordinates $06^h45^m11.2^s \leq RA \leq 06^h45^m59.4^s$ and $-01°27'21'' \leq \delta \leq +01°6'23''$ (J2000) in the Monoceros constellation, towards Galactic anti-center direction.

Fifty-one transit candidates have been identified in LRa01 (Tables 5 and 6). Four transiting planets have been discovered and confirmed: *CoRoT*-5b (Rauer et al. 2009), *CoRoT*-

12b (Gillon et al. 2010), and CoRoT-21b (Pätzold et al. 2011), three Jupiter-size planets with M_p = 0.47, 0.92, and $\approx 2\,M_{Jup}$, respectively; *CoRoT*-7b, the first terrestrial transiting planet (Léger et al. 2009; Queloz et al. 2009). A non-transiting planet with a mass of about $8\,M_{Earth}$ in the *CoRoT*-7-system, namely *CoRoT*-7c, was also detected by radial velocity (RV) observations only (Queloz et al. 2009). The potential discovery of a third planet in the *CoRoT*-7-system, *CoRoT*-7d, was reported by Hatzes et al. (2010). A list of photometrically identified binary systems is presented in the Table 7. Identified variable stars of the first four *CoRoT* exoplanet star fields are reported in Debosscher et al. (2009).

The present work reports on the characteristics of the LRa01 star-field (Section 2), the *CoRoT* photometry and nature of different instrumental systematic effects (Section 3), the transit detection (Sections 4), and the observing strategy of ground-based follow-ups (Section 5). The process of resolving the nature of *CoRoT* candidates is described in Moutou et al. (2009). A description of all the detected transit candidates is presented in Section 6. Results are discussed in terms of detection efficiency compared to previous *CoRoT* runs (Section 7). At the end of the manuscript, a summary is also reported (Section 8).
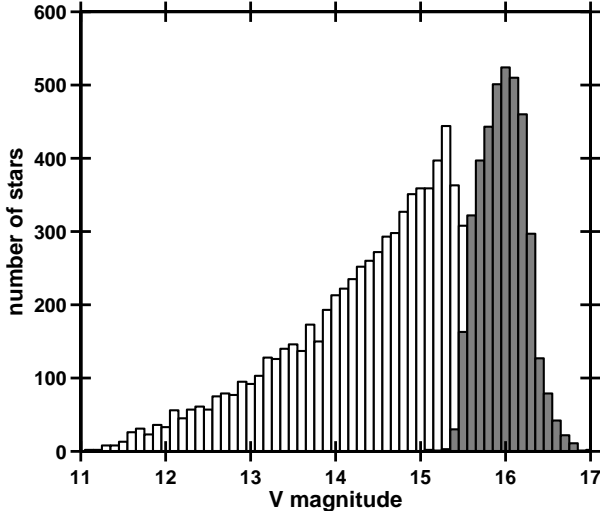
Fig. 1. Histogram of the the visual magnitudes of the stars observed by *CoRoT* in the LRa01 exoplanet star field. Gray: monochromatic lightcurves. White: chromatic lightcurves. The majority of the targets are relatively faint stars with $V > 14$ mag.

2. Field characterisation

During the *CoRoT* mission preparatory phase, a massive and deep Harris *BV* and Sloan *r'i'* photometric survey was performed in the *CoRoT* exoplanet fields using the Wide Field Camera (WFC) at the Isaac Newton Telescope (INT). The goals were i) to perform a first-order spectral classification of the stars in the fields, ii) to determine their position with sufficient accuracy for a precise placement of the *CoRoT* photometric masks, and iii) to assess the level of contamination from background/foreground objects within a few arc-seconds from the *CoRoT* target stars. The relevant information is collected in the Exo-Dat database[1] (Deleuil et al. 2006, 2009; Meunier et al. 2007).

CoRoT was designed to fulfil two main objectives: conducting stellar seismology studies of interesting stars and searching for extrasolar planets. Astroseismology requires high signal-to-noise (S/N) ratio photometry and it is thus focused mainly on the study of relatively bright targets: typically ~10 stars with $V<9.5$ mag are observed in each *CoRoT seismo*-field. On the other hand, the transiting exoplanet search requires a large number of targets because of the low probability to find planets whose orbits are oriented such that transits can be observed in front of their host stars (the probability is about 5 % for semi major axes of 0.1 AU). The selection of the observed *CoRoT seismo*- and *exo*-fields thus represent a compromise between these two requirements.

11 408 stars with visual magnitudes $11 \lesssim V \lesssim 17$ mag were observed for the transit search in the LRa01 field (Figure 1). Dwarf stars are optimal targets for the photometric search of extrasolar planets (Michel et al. 2008; Gondoin et al. 2009; Hekker et al. 2009). Therefore, the percentage of Sun-like stars in a field is important to estimate the detection efficiency. Combining the Exo-Dat optical photometry (Deleuil et al. 2009) with the near-infrared Two Micron All Sky Survey (2MASS) Point Source catalog[2] (Cutri et al. 2003) and using color-
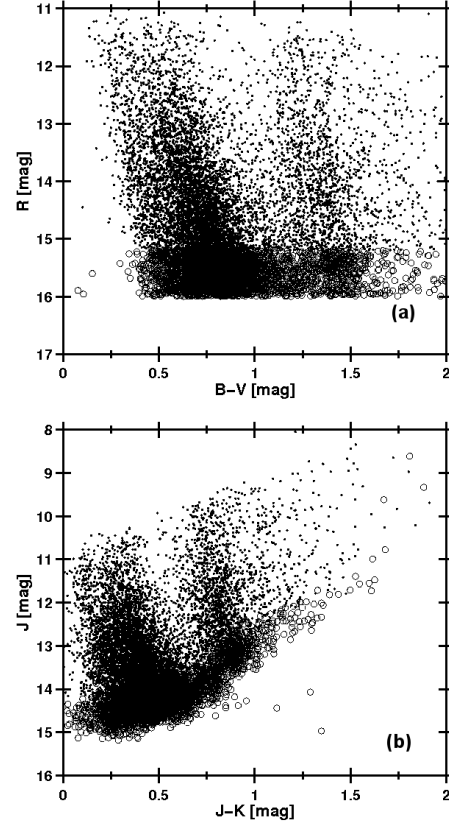
---

[1] http://lamwws.oamp.fr/exodat/
[2] The near-infrared *JHKs* 2MASS catalogue is available at http://irsa.ipac.caltech.edu/applications/2MASS/IM/interactive.html.

Fig. 2. *Top panel*: r' versus $B - V$ color-magnitude diagram of the stars in the *CoRoT* LRa01 star field. The dots mark the bright stars ($r' \lesssim 15.2$ mag), for which three-color *CoRoT* lightcurves are available. The open circles mark the fainter stars ($r' \gtrsim 15.2$ mag) with monochromatic lightcurves only. Main sequence stars cluster in the left part of the diagram, giant stars in the right part. *Bottom panel*: 2MASS J versus $J - Ks$ color-magnitude diagram of the stars in the *CoRoT* LRa01 field. Again, main sequence stars cluster in the left part of the diagram, giant stars in the right part.

magnitude diagrams (Figure 2), the percentage of giant and dwarf stars in LRa01 is estimated. Although it is difficult to find a clear distinction between these two populations using broadband photometry (in particular for stars with $V \gtrsim 15$ mag), 75 % of the stars observed by *CoRoT* in LRa01 seem to be dwarf stars (Figure 2). The distribution of luminosity classes derived from Exo-Dat only shows a similar picture (Figure 3): less than 0.05 % of the stars in the LRa01 star field are supergiants, less than 0.2 % are bright giants, ~24 % are giants, ~13 % are sub-giants, and ~62 % are dwarf stars. This is of advantage for the search of extrasolar planets compared to the LRc01 star field, where ~58 % of the stars are giant stars (Cabrera et al. 2009). However, this analysis is valid on a statistical point of view. Photometric criteria can indeed lead to misclassification of individual stars (see Klement et al. 2011, and reference therein). The Exo-Dat spectral classification, based only on broad-band photometry, suffers some uncertainties, the main ones being the star reddening, the unknown chemical abundances, and the potential binarity which can result in a wrong identification of the spectral and luminosity classes of the stars. Based on multi-object, intermediate-resolution spectroscopy performed with FLAMES@VLT on a sub-set of stars

Fig. 4. Phase-plot of the candidate LRa01 E2 2597 (*CoRoT* ID 0102672065) folded at the period $P = 8.90$ days in the three color channels red (star), green (circle), and blue (diamond). The lightcurves are normalised to the fluxes in the respective colors. The event is only visible in the blue channel. This indicates a contamination from a background binary system.
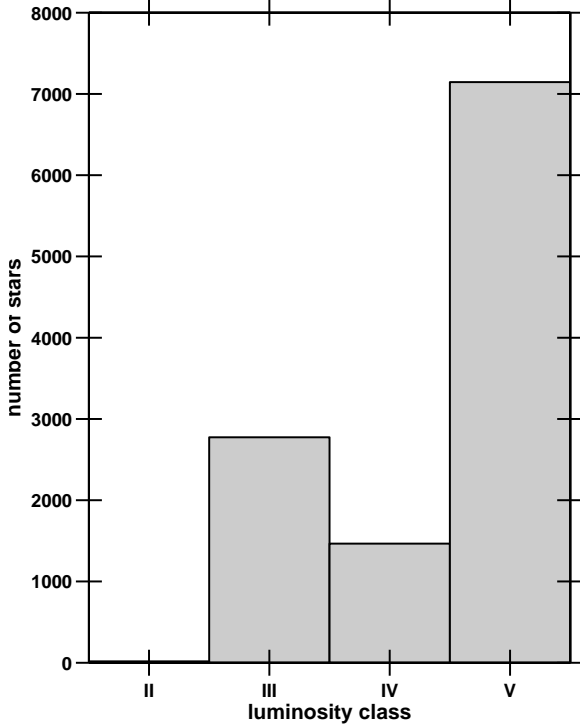
Fig. 3. Histogram of the luminosity classes of the LRa01 star field as derived from Exo-Dat (Deleuil et al. 2009). The majority of the target stars ($\sim 62\,\%$) are main sequence dwarf stars (luminosity class V). Sub-giant (luminosity class IV), giant (luminosity class III), and bright giant stars (luminosity class II) make up ~13, ~24, <0.2 % of the total, respectively. Super-giant stars (luminosity class I; not reported in the histogram) make up <0.05 %.

in LRa01, Gazzano et al. (2009) found that the photometrically classified dwarf content is underestimated by about 15 %.

3. *CoRoT* photometry, data reduction, and systematic effect

CoRoT data are made public after a proprietary period of one year. The data from LRa01 were released to the CoIs on 29 October 2008 and to the public on 29 October 2009. *CoRoT* lightcurves are identified by either the *CoRoT* ID, a unique 10 digit number, or the so-called *CoRoT* "Win ID" (i.e., window ID). The "Win ID" contains the identifier E1 or E2, which identifies the CCD 1 or 2 of the exoplanet channel, respectively, followed by a 4-digit number. This number represents the assigned *CoRoT* mask. The "Win ID" is re-used for every run. To identify an individual lightcurve by the "Win ID", the data acquisition run is required. In addition, a three character abbreviation, MON or CHR, is given for the identification of chromatic or monochromatic lightcurves, respectively. For example, the lightcurve of the star *CoRoT*-7, observed during LRa01 and harbouring the first transiting terrestrial planet (Léger et al. 2009), is labeled by the following identification: LRa01 E2 0165 - CHR - 0102708694.

A bi-prism was installed in the exoplanet channel to disperse the flux of the observed stars. Three-color photometry is obtained by splitting the point-spread function into three sub-
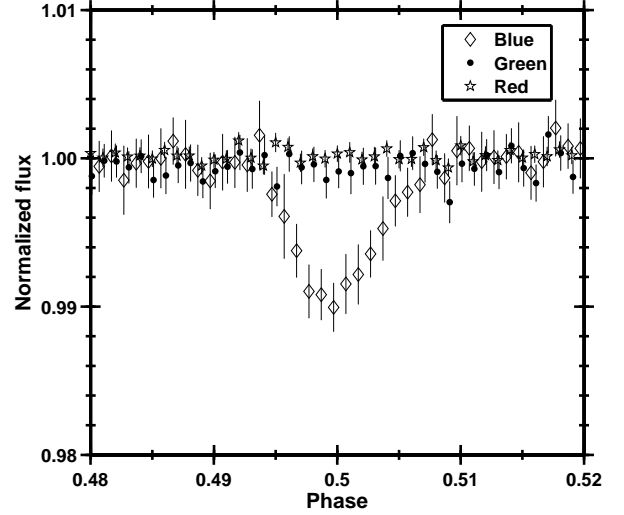
areas based on the dispersion property of the bi-prism (blue light is stronger dispersed than red light) for the targets with visual magnitudes $V \lesssim 15.2$ mag, i.e., about 65 % of the lightcurves in this run. Flux from these areas is defined as red, green, and blue. The *CoRoT* color channels, however, do not correspond to any standard photometric systems (Auvergne et al. 2009).

The chromatic information is helpful to distinguish between achromatic planetary transits and chromatic eclipsing binaries. The chromatic information is also used to identify false alarms from diluted background binaries. After an accurate study of the light contamination inside the photometric mask, candidates with 3 sigma significant depth differences in the three *CoRoT* channels are usually flagged as potential contaminating eclipsing binaries. As an example, the *CoRoT* target LRa01 E2 2597 has a deep transit in the blue channel[3] which is not detected, neither in the green channel nor in the red channel, at a $12\,\sigma$ and $25\,\sigma$ significance, respectively (Figure 4). If the signal were on target the respective transit depths in the red and green channel would have been clearly detected. As a consequence, this candidate is identified as a contaminating eclipsing binary (CEB). In other cases, i.e., LRa01 E1 2101 (Section 6.3.2) and LRa01 E2 3156 (Section 6.3.13), the signal is detected in only one channel but the expected signal strengths in the other channels is below the noise threshold. Therefore, we could not exclude such signals as arising from a contaminanting eclipsing binary. Indeed, ground-based photometric follow-up concluded that the transit signal of LRa01 E1 2101 and LRa01 E2 3156 are likely on target.

Several systematic effects need to be filtered out during the data reduction to achieve maximum accuracy. The main perturbating factors are eclipses (when the spacecraft enters the shadow of the Earth) which cause short-term temperature fluctuations on the spacecraft, the Earth's gravity and magnetic field, solar and terrestrial infrared emissivity, the Earth's

---

[3] 1 % deep when normalized to the blue flux only, 0.14 % deep when normalized to the total flux of all three channels.

albedo, and objects in low-Earth orbit. Known instrumental effects like spacecraft jitter are already removed in the processing. A detailed description of lightcurve perturbations and employed corrections is given in Auvergne et al. (2009), and Drummond et al. (2008) and Pinheiro da Silva et al. (2008), respectively. Details about on board data-reduction can be found in Llebaria & Guterman (2006).

Irradiation excites single pixels, which are difficult to correct. These "hot-pixels" appear predominantly in orbit when crossing the South Atlantic Anomaly (SAA). A value in the header of each lightcurve informs the user how many "hot-pixels" were identified in the lightcurve. Not all "hot-pixels" are identified during the data processing. Unfortunately, these events may mimic a transit-like signal. If only one pixel is affected, this can be identified by comparing the flux in the different color channels (if available).

Although the processing pipeline reduces significantly the noise and removes the systematics, some instrumental effects still remain. As an example, the three color-channel lightcurves of the star LRa01 E1 2698 (*CoRoT* ID 0102566329), are plotted in Figure 5. Instrumental signatures significantly perturb the lightcurve. On 2454433 HJD ($T_{jump,blue}$ = 2888 days on Figure 5) a strong "hot-pixel" appeared in the blue channel. It perturbed the white lightcurve only weakly since the flux contribution from the blue channel was small. On 2454465 HJD ($T_{jump,red}$ = 2920 days on Figure 5) a small "hot-pixel" appeared in the red channel. The effect is seen in the white lightcurve with almost the same amplitude because the red channel contributes most to the overall flux. It should also be noted that the relaxation time for this "hot-pixel" is very short compared to the strong event in the blue channel. The flux after the incident settles on a slightly higher level than before. This example proves the usefulness of chromatic data to identify "hot-pixels".

There is a data gap of 3.68 days between HJD 2454484 and 2454488 ($T_{data gap}$ = 2939 − 2943 days on Figure 5). A proton impact led to a reset of the Data Processing Unit (DPU) 1, which is responsible for data collection on the E1 CCD, on 18 January 2008 at 22:45:57 UT during the SAA crossing. The recording resumed on 22 January 2008 at 14:37:41 UT. All lightcurves in LRa01 originating from CCD 1 contain this data gap.

In order to correct for the effects not removed by the *CoRoT* pipeline, each detection team inside the *CoRoT* exoplanet team uses a set of additional filters before applying the transit search algorithms. A description of the various methods applied by each detection team to analyse the *CoRoT* lightcurves is given in Alapini & Aigrain (2008); Bordé et al. (2007); Carpano & Fridlund (2008); Moutou et al. (2005, 2007); Régulo et al. (2007); Renner et al. (2008); Grziwa et al. (2011).

4. Detection of *CoRoT* candidates

The transit candidate selection for each run is performed twice: by the "Alarm Mode", during the on-board observation, and by the *CoRoT* detection teams, after completion of the on-board observation and the full reduction of the *CoRoT* data.

The "Alarm Mode" checks for planetary transits every two weeks, when the *CoRoT* observations are still ongoing (Surace et al. 2008). If the "Alarm Mode" detects a promising candidate with a planetary transit-like event, the sampling for this specific lightcurve is increased from 512 to 32 seconds. A preliminary candidate list is created and the candidate coordinates, along with estimated transit properties, are forwarded to the follow-up teams who perform the ground-based observation campaign (Section 5). A dedicated analysis and transit search is
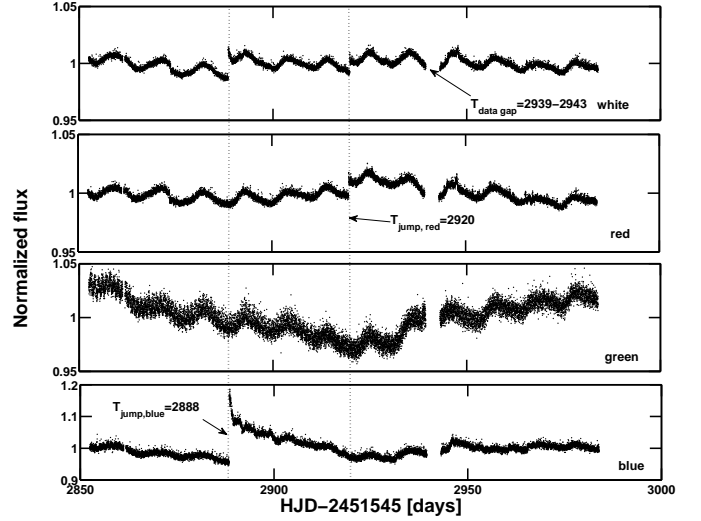

Fig. 5. Chromatic lightcurves of the star LRa01 E1 2698. From top to bottom: white (red + green + blue), red, green, and blue lightcurve versus observing time in HJD. The flux of each lightcurve is normalized to 1. The red channel contributes the most to the combined white lightcurve (79 % of the flux). 10 % of the combined white flux originates from the green channel, whereas the blue channel contributes 11 % of the total white flux. The dashed lines mark the position of two small "hot-pixels" in the blue and red channels that can also be found in the white lightcurve.

performed when the processed data are distributed to the different detection teams within the *CoRoT* Exoplanet Science Team (typically several months after the end of the *CoRoT* observation).

The detection teams benefit from the total temporal length of the lightcurves (about 130 days for LRa01) and the reduced noise after full processing, and are well equipped for finding shallow transits around highly variable and active stars. The detection teams try to sort out as many false positives as possible in order to avoid the waste of observation time and telescope resources on non-planetary objects (Section 5). See Cabrera et al. (2009) for a full description of the *CoRoT* detection pipeline, with the generation of an initial candidate list and subsequent vetting for the presence of false alarms arising from eclipsing binaries. In the end, a prioritised list of planet candidates and their parameters is composed, which is subject to further follow-up observations.

The list of the LRa01 candidates is given in Table 5, along with coordinates, transit period, epoch, duration and depth. Each candidate is described in detail in Section 6.

5. Ground-based follow-up observations of the *CoRoT* candidates

The detection of planetary transit candidates in the *CoRoT* lightcurves is only the start on a long, and time consuming *road* to the successful confirmation of the planetary nature. The *CoRoT* follow-up is done with ground based facilities, following the strategy outlined in Alonso et al. (2004). Ground-based follow-up observations are motivated by the need to exclude false positives from the list of candidates and to obtain a full characterisations of the detected planets. Practically all

Table 1. Instruments used for the ground-based *CoRoT* follow-up observations.

Instrument	Observatory
Photometry	
CAMELOT on the IAC 80 cm telescope; SD camera on the ESA Optical ground-station (ESA-OGS); FastCam at the Carlos Sanchez Telescope (CST)	Observatorio del Teide, Canary Islands, Spain
CCD cameras on the 0.46 m and 1 m Wise telescopes	Wise Observatory, Israel
EulerCam on the Euler 1.2 m telescope	La Silla observatory, Chile
MegaCam on the 3.6 m Canada-France-Hawaii telescope (CFHT)	CFH observatory, Hawaii, USA
CCD camera on the 1.2 m MONET-North telescope	McDonald Observatory, Texas, USA
NACO on the ESO's VLT	Paranal Observatory, Chile
BEST on the DLR 20 cm telescope	Observatoire de Haute-Provence (OHP), France
BEST II on the DLR 25 cm telescope	Observatorio Cerro Armazones, Chile
Spectroscopy	
AAOmega on the 3.9 m AAO telescope	Anglo-Australian Observatory, Australia
FLAMES-GIRAFFE and UVES on ESO's VLT	Paranal Observatory, Chile
CRIRES on ESO's VLT	Paranal Observatory, Chile
CORALIE on the 1.2 m Euler telescope, HARPS on the ESO 3.6 m telescope	La Silla observatory, Chile
SANDIFORD on the 2.1 m Otto Struve telescope	McDonald Observatory, Texas, USA
Coudé spectrograph on the 2 m TLS telescope	Thüringer Landessternwarte (TLS), Tautenburg, Germany
SOPHIE on the 1.93 m telescope	Observatoire de Haute-Provence (OHP), France
HIRES on the 10 m Keck I telescope	Keck observatory, Hawaii,USA
FIES on the 2.56 m NOT telescope	Roque de los Muchachos Observatory, Canary Islands, Spain

false positives in transit searches are due to some configuration involving eclipsing binary systems, with the large majority of false positives caused by either grazing or diluted eclipsing binaries (Section 5.2). Their nature was first described by Brown (2003), with a development for CoRoT candidates given by Almenara et al. (2009).

Photometric observations are needed to confirm that the transit is occurring 'on target' (Section 5.1). If confirmed, complementary RV observations are performed to definitely assess the planetary nature of the transiting body and eventually reveal the true mass of the planet. High S/N ratio spectroscopy at high-resolution are also conducted to derive the photospheric fundamental parameters of the planet host star and determine its mass and radius (Section 5.2).

The *CoRoT* follow-up program is challenging both in terms of telescope capabilities and observation time. The *CoRoT* follow-up community uses time allocated at different observatories as described in Sections 5.1 and 5.2. Many RV observations in 2008 and 2009 were dedicated to *CoRoT*-7 in order to confirm the existence and nature of the companions and to constrain their parameters (Léger et al. 2009; Queloz et al. 2009; Hatzes et al. 2010, 2011). Follow-up observations for other candidates were therefore limited or delayed to the 2009/2010 and 2010/2011 observing season. Table 1 lists all facilities used for the follow-up of the LRa01 candidates, Table 6 lists the results of the follow-up in a concise form. Details can be found in the description of the individual candidates in Section 6.

5.1. Photometry

The first step in the follow-up sequence is the ground-based photometric observation of the transit. It needs to be verified that the detected transit signals occur on the main target inside the *CoRoT* photometric mask (typically 20″ large). The star is observed during a transit, and again between two transits. The stellar brightness, as well as that of any other nearby star is monitored. Contaminating eclipsing binaries (CEBs) are sorted out by this procedure. The method is described in more detail in Deeg et al. (2009).

Required for these observations is the correct and precise prediction of the epoch of the transit occurrence. Timing errors of more than a few hours make the follow-up of transit events unfeasible. The ephemeris errors of faint or shallow candidates (listed in Table 5) imply that their follow-up has to be performed within 1-2 years after *CoRoT* on-board observation.

As part of the photometric follow-up program of *CoRoT*, the BEST telescope at OHP performed a survey of variable stars in the LRa01 field prior to the satellite launch (Kabath et al. 2008). The eclipsing binaries LRa01 E1 1574 and LRa01 E1 0622 (Table 7) are among the targets previously found in the aforementioned paper.

5.2. Spectroscopy

The conclusion on the nature of some transiting objects is drawn from complementary time-series RV measurements as well as high-resolution, high S/N ratio spectroscopy.

RV measurements are required to reject possible false-positives and confirm the planetary nature of the transiting object. Binary system, eventually identified by RV measurements, are classified into the following categories: i) binaries with only one stellar component spectroscopically visible (SB1); ii) binaries with two or more stellar components spectroscopically visible (SB2, SB3, etc.); iii) blended eclipsing binary, i.e., spatially unresolved eclipsing binary whose light is diluted by the main *CoRoT* target (blend).

Transits provide the direct measurement of the planet-to-stellar radius ratio (R_P/R_*), whereas RV measurements yield the

mass function of the star/planet system. Stellar radii and masses are thus needed to determine radii and masses of the transiting candidates. A first-oderder estimate of the size of the transiting objects is derived from the spectral types of the host-stars, as listed in the Exo-Dat data-base. However, as already described in Section 2, the photometrically spectral classification reported in Exo-Dat suffers some uncertainties. High-resolution, high S/N ratio spectroscopy is thus necessary to derive stellar mass and radius and, eventually, determine the mass, radius, and bulk density of the confirmed planets.

The spectroscopic follow-up observations of LRa01 started with a first spectroscopic "snap-shot" of some of the *CoRoT* candidates. Low-resolution ($R \approx 1\,300$) reconnaissance spectroscopy was performed with the AAOmega multi-fiber spectrograph mounted at the 3.9 m telescope of the Australian Astronomical Observatory (AAO) during two observing runs, in January 2008 and from December 2008 to January 2009. Further multi-object spectroscopic observations were performed with the FLAMES-GIRAFFE facility ($R \approx 26\,000$) at the ESO Very Large Telescope (Paranal Observatory, Chile) in winter 2005 (Loeillet et al. 2008; Gazzano et al. 2009).

The AAOmega and FLAMES-GIRAFFE observations classified the stars and derived a fist estimate of their photospheric parameters as described in Gandolfi et al. (2008) and Gazzano et al. (2009). If the host star turned out to be a giant star, although it was listed as a main sequence star in the Exo-Dat database, the size of the transiting object was re-evaluated based on the new stellar parameters. Planned ground-based photometry and RV follow-up observations were cancelled if the size of the transiting body was inconsistent with a planetary object. This spectroscopic screening singled out also B-type stars and rapidly rotating targets for which high-precision RV measurements are not feasible.

The nature of the transiting objects is further investigated through reconnaissance high-resolution spectroscopy. This is performed using the CORALIE spectrograph at the 1.2 m Euler telescope in La Silla observatory, the Sandiford cassegrain echelle spectrograph on the 2.1 m telescope at McDonald Observatory, and the coudé echelle spectrograph of the 2 m telescope of the Thüringer Landessternwarte (TLS). If this stage is successfully passed, the planetary candidate is handed down to SOPHIE at the 1.93 m telescope at the Observatoire de Haute-Provence (OHP). In its high efficiency mode ($R \approx 40\,000$), SOPHIE is able to reach RV precision of a few dozen m s^{-1} on a solar-like star, down to $V \approx 14.5$ mag. This accuracy is fully sufficient for detecting Jupiter-like, and even Saturn-like planets, in a close-in orbit around a solar-like star. We recently took also advantage of the fiber-fed FIES spectrograph attached at the 2.56 m Nordic Optical Telescope (NOT). The recent refurbishments carried out at this instrument had improved the capability of FIES for very high-precision RV measurements down to ~ 10 m s^{-1}, making this spectrograph a precious resource to use for *CoRoT* RV follow-up.

The final "step" of the RV follow-up uses high-precision RV measurements with HARPS at ESO's 3.6 m telescope. The RV follow-up of the faintest candidates in LRa01 ($15 \lesssim V \lesssim 16$ mag) has been strengthened using the HIRES echelle spectrograph on the 10 m Keck I telescope.

The photospheric parameters of the candidates, i.e., effective temperature ($T_{\rm eff}$), gravity ($\log g$), metallicity ($[M/H]$), and projected rotational velocity ($v \sin i$), are usually derived by analysing also the acquired high-resolution spectra, as already described in other *CoRoT* exoplanet papers (e.g., Deleuil et al. 2008; Léger et al. 2009; Bruntt et al. 2010; Gandolfi et al. 2010).

Stellar masses and radii are then inferred by comparing the location of the objects on a $T_{\rm eff}$ *vs.* $\log g$ diagram with theoretical evolutionary tracks. Only an estimate of the spectral type can be derived for candidates with low S/N ratio spectra (<10-15), as described in some cases in Section 6.

For the confirmed planetary candidates high S/N ratio spectra are usually acquired with HARPS, HIRES, and UVES (ESO, Paranal Observatory) spectrographs.

6. *CoRoT* planetary candidates

Here we present the *CoRoT* transit candidates along with a brief overview over the properties of the star and the detected transit signal. Any follow-up observations that have been performed are also described. The candidates are presented in the following order: confirmed planets, identified non-planetary objects, unsettled good planetary candidates, unsettled low priority planetary candidates (suspected binaries), false alarms, and the so-called "X-case" candidates (see below).

A planet is considered confirmed when RV-measurements definitely assess the planetary nature of the transiting object and allow to determine its mass (Section 6.1). Candidates listed as "settled cases - non planetary objects" (Section 6.2) are objects whose non planetary nature were identified by either photometric or spectroscopic follow-up observations. These include blends, contaminating eclipsing binaries (CEB), and binary systems.

Most of the observing time reserved for LRa01 was invested on *CoRoT*-7. Therefore many candidates were being followed-up in the 2009/2010 and some even in the 2010/2011 observing seasons. Still, follow-up observations could not be concluded for all candidates. These are listed as unresolved cases and are subdivided into "unsettled good planetary candidates" (Section 6.3) and "unsettled low priority planetary candidates" (Section 6.4), based on the analysis of the *CoRoT* lightcurves only. The latter were usually not followed-up due to one or more bad characteristics hinting at stellar binary scenario (e.g., out of transit variations, depth differences between even and odd transits or different color channels, very shallow secondary eclipse).

For the sake of completeness "false alarm" objects are also included (Section 6.5). These are shallow transit candidates that were identified by one detection team in lightcurves heavily affected by instrumental effects. They are considered as probable false alarms because they could not be reproduced by other detection teams using different filtering techniques. The "X-case" candidates (Section 6.6) are objects that might be planetary candidates if the spectral type of the target star were considerable different than the one listed in Exo-Dat. They have a very low priority in the follow-up program and were not observed so far. Finally, in some cases only a single transit event is present in the *CoRoT* lightcurve. Those are listed as "mono-transits" (Section 6.7). The depth of the signals indicates that these are eclipsing stellar binaries (Table 7).

A concise list of the transit parameters and the follow-up status of the candidates can be found in Tables 5 and 6, respectively. The RV-measurements performed on the *CoRoT* LRa01 candidates are listed in Table 4. For the RV data of the confirmed exoplanets in LRa01, we refer the reader to the respective articles reporting on their discovery.

6.1. Confirmed planets

Four candidates detected during the *CoRoT* LRa01 run were confirmed as *bona fide* transiting planets (see Table 2 for

Table 2. Parameters of the planets detected in the *CoRoT* LRa01 field.

Planet	Host star spectral type	Planetary mass	Planetary radius	Semi-major axis [AU]	Source
CoRoT-7b	G9V	$4.8 \pm 0.8\,M_{Earth}$	$1.68 \pm 0.09\,R_{Earth}$	0.0172 ± 0.0002	Léger et al. (2009); Queloz et al. (2009)
	G9V	$6.9 \pm 1.5\,M_{Earth}$	$1.68 \pm 0.09\,R_{Earth}$	0.0172 ± 0.0002	Léger et al. (2009); Hatzes et al. (2010)
	G9V	$5.2 \pm 0.8\,M_{Earth}$	$1.58 \pm 0.10\,R_{Earth}$	0.0172 ± 0.0002	Queloz et al. (2009); Bruntt et al. (2010)
	G9V	$2.3 \pm 1.8\,M_{Earth}$	$1.58 \pm 0.10\,R_{Earth}$	0.0172 ± 0.0002	Pont et al. (2011); Bruntt et al. (2010)
	G9V	$8.0 \pm 1.2\,M_{Earth}$	$1.58 \pm 0.10\,R_{Earth}$	0.0172 ± 0.0002	Ferraz-Mello et al. (2011); Bruntt et al. (2010)
	G9V	$5.7 \pm 2.5\,M_{Earth}$	$1.58 \pm 0.10\,R_{Earth}$	0.0172 ± 0.0002	Boisse et al. (2011); Bruntt et al. (2010)
	G9V	$7.42 \pm 1.21\,M_{Earth}$	$1.58 \pm 0.10\,R_{Earth}$	0.0172 ± 0.0002	Hatzes et al. (2011); Bruntt et al. (2010)
CoRoT-7c*	G9V	$8.4 \pm 0.9\,M_{Earth} \sin i$	-	0.046	Queloz et al. (2009)
	G9V	$12.4 \pm 0.4\,M_{Earth} \sin i$	-	0.045	Hatzes et al. (2010)
	G9V	$13.6 \pm 1.4\,M_{Earth} \sin i$	-	0.045	Ferraz-Mello et al. (2011)
	G9V	$13.2 \pm 4.1\,M_{Earth} \sin i$	-	0.045	Boisse et al. (2011)
CoRoT-7d*	G9V	$16.70 \pm 0.42\,M_{Earth} \sin i$	-	0.080	Hatzes et al. (2010)
CoRoT-5b	F9V	$0.467^{+0.047}_{-0.024}\,M_{Jup}$	$1.388^{+0.046}_{-0.047}\,R_{Jup}$	$0.04947^{+0.00026}_{-0.00029}$	Rauer et al. (2009)
CoRoT-12b	G7V	$0.917 \pm 0.07\,M_{Jup}$	$1.44 \pm 0.13\,R_{Jup}$	0.0402 ± 0.0009	Gillon et al. (2010)

* *CoRoT*-7c and *CoRoT*-7d were detected by RV measurements only. The real nature of *CoRoT*-7d of is not definitely assessed. See Pätzold et al. (2011) for the parameters of CoRoT-21b.

the full parameters). Three Jupiter-sized planets, *CoRoT*-5b (Rauer et al. 2009), *CoRoT*-12b (Gillon et al. 2010), and *CoRoT*-21b (Pätzold et al. 2011), and the first transiting terrestrial planet *CoRoT*-7b (Léger et al. 2009; Queloz et al. 2009). For the very first time, the bulk density of a small extrasolar planet was derived consistent with the bulk densities of terrestrial planets (see Table 2). An accurate reanalysis of the acquired HARPS and UVES spectra was recently published by Bruntt et al. (2010), leading to an improvement of stellar parameters of *CoRoT*-7.

There are now a number of independent determinations of the mass of CoRoT-7b. See Table 2 and Hatzes et al. (2011) for a detailed discussion. We note that CoRoT-7b is almost identical to the recently discovered transiting Super-Earth Kepler-10b. Kepler-10b has a period of about $P = 0.84$ days, mass $M_P = 4.56^{+1.17}_{-1.29}\,M_{Earth}$, radius $R_P = 1.416^{+0.033}_{-0.036}\,R_{Earth}$, and mean density $\rho = 8.8^{+2.1}_{-2.9}\,\mathrm{g\,cm^{-3}}$ (Batalha et al. 2011).

CoRoT-7b is the only transiting planet in the *CoRoT*-7b system. Two other planets are inferred from RV measurements only: Queloz et al. (2009) discovered *CoRoT*-7c; Hatzes et al. (2010) found evidences of the presence of a third planet, *CoRoT*-7d (see also Table 2), but further RV measurements are required to definitely assess its planetary nature. The detection of these two additional planets is disputed by Pont et al. (2011).

CoRoT-21b, also known as candidate LRa01 E2 5277 (*CoRoT* ID 0102725122), has been recently confirmed as a transiting hot-Jupiter planet. The lightcurve of its faint host star ($V = 16.1\,\mathrm{mag}$) contains a 0.45 % deep transit signal with a period of 2.73 days (Figure 6). Photometric follow-up observations performed with IAC80 confirm the transit event on target. RV measurements conducted with HARPS, and recently with HIRES, show significant variations in phase with the

CoRoT ephemeris and consistent with a $\sim 2\,M_{Jup}$ planet around a F8 IV star ($T_{\mathrm{eff}} \approx 6100\,\mathrm{K}$, $log\,g \approx 3.5\,\mathrm{dex}$). Since the parameters of CoRoT-21b are still under investigation, the planet is not listed in Table 2 but in Tables 5 and 6. It will be presented in a forthcoming paper (Pätzold et al. 2011), along with the HARPS and HIRES RV measurements.

6.2. Settled cases: non planetary objects

The following objects are identified as non-planetary objects based on ground-based follow-up observations.

6.2.1. LRa01 E1 0544 - CHR - 0102714746

LRa01 E1 0544 is a relatively bright star ($V = 13.39\,\mathrm{mag}$) with a 0.15 % deep eclipse occurring every 2.75 days. AAOmega observations classify the target as a F7 dwarf star, in good agreement with the classification listed in Exo-Dat (F8 IV). SOPHIE spectroscopic observations indicate a fast rotator with no significant RV variations down to a precision of $50\,\mathrm{m\,s^{-1}}$. EulerCam measurements show no transit events on target. Instead a ~ 4 magnitude fainter star located 9″ West of the main target has deep eclipses ($D \approx 20\,\%$). IAC80 observations confirm this result. This object is a contaminating eclipsing binary (CEB).

6.2.2. LRa01 E1 0561 - CHR - 0102597681

This is a relatively bright candidate ($V = 12.00\,\mathrm{mag}$) listed as a SpT=A0 V star in Exo-Dat. The *CoRoT* lightcurve shows a 0.70 % deep transit occurring every 20.82 days superimposed on a γ-Doradus like pulsations. Low-resolution AAOmega spectroscopy classifies this object as a A7 IV/V star. Two moderate
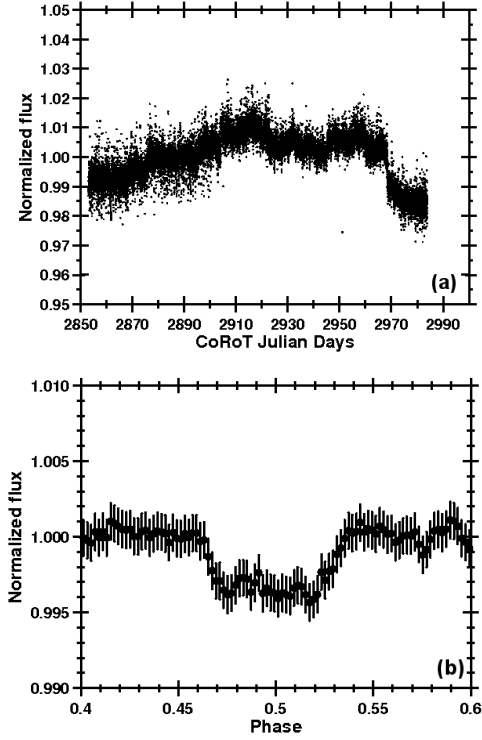
Fig. 6. *Top panel*: Raw white lightcurve of LRa01 E2 5277 (also known as *CoRoT*-21b). *Bottom panel*: Normalized and phase-folded raw white lightcurve of the transit candidate LRa01 E2 5277 at the transit period $P = 2.73$ days. A baseline fit has been subtracted around each transit before folding.

Fig. 7. The HARPS RV measurements of LRa01 E1 5015 (points) phased to the *CoRoT* transit period ($P = 13.69$ days) and epoch. The best fitting sine curve is over-plotted with a line. Note that the systemic velocity has been subtracted.

6.2.5. LRa01 E1 5015 - MON - 0102777869

This is a candidate around a relatively faint ($V = 16.17$ mag) G2 V star (Exo-Dat) with a 1 % deep transit signal and a period of 13.69 days. The long transit duration of about 10 hours implies an eclipsing binary.

ESA-OGS observations show that the transit is on target. Figure 7 reports the HARPS RV measurements of LRa01 E1 5015 phase folded to the *CoRoT* transit period and epoch, along with a sine fit. The semi-amplitude is $K = 16.5$ km s^{-1} which corresponds to a mass function[4] $f(m) = 0.00637\,M_\odot$. Assuming a mass of $1\,M_\odot$ for the main component, the companion mass is $\approx 0.18\,M_\odot$. This is a SB1 system with a low-mass companion star.

6.2.6. LRa01 E1 4353 - MON - 0102692038

This candidate in the lightcurve of a $V = 15.78$ mag star of spectral type A5 V (Exo-Dat) has 1.09 % deep eclipse with a period of 5.23 days. EulerCam on-off photometry shows a constant flux in the target but a 5 % deep eclipse in a contaminant star (*CoRoT* ID: 0102691690, $V = 16.7$ mag). IAC80 confirms the EulerCam observations. This is a contaminating eclipsing binary (CEB).

6.2.7. LRa01 E2 1123 - MON - 0102615551

A 1.80 % deep signal with a period of 3.88 days is detected in the *CoRoT* lightcurve of this candidate. IAC80 and Wise photometry confirms the transit signal is on target. UVES and HARPS observations of this $V = 14.62$ mag object identify the target as a K5 dwarf star instead. Two CORALIE and six HARPS RV measurements show no significant sinusoidal variations with an amplitude greater than ~ 50 m s^{-1}.

An examination of the Ca II H & K region from spectra taken with UVES shows three emission components. The RVs of two

S/N≈ 35 ratio SOPHIE spectra reveal a low-contrast single peak cross-correlation function (CCF) with a RV variation of about 52 km s^{-1}, in anti-phase with the *CoRoT* ephemeris, i.e., the eclipses occur on the rising part of the RV curve and are caused by the star whose CCF peak is detected in the SOPHIE spectra. A single epoch UVES spectrum with higher S/N ratio (~ 120) unveils the presence of other two components in the system, making the candidates a spectroscopically resolved SB3 system with pulsating components.

6.2.3. LRa01 E1 2890 - MON - 0102618931

According to Exo-Dat, this candidate has an apparent V-magnitude of 15.73 and its spectral type is G5 III. IAC80 on-off photometry shows that a contaminating eclipsing binary is the origin of the transit signal in this lightcurve ($D = 0.29\,\%$, $P = 2.43$ days). It is ~ 3.2 mag fainter than the target and positioned $\sim 12''$ South-East from LRa01 E1 2890.

6.2.4. LRa01 E1 3666 - MON - 0102790970

This is a faint ($V = 15.47$ mag) F5 V star (Exo-Dat) with an apparent transit signal of 0.45 % depth and a period of 1.55 days. CFHT and IAC80 observations identify a nearby background star $\sim 8''$ West of the target with a variation of 1.5 % as the source of the signal. The candidate is a contaminating eclipsing binary (CEB).
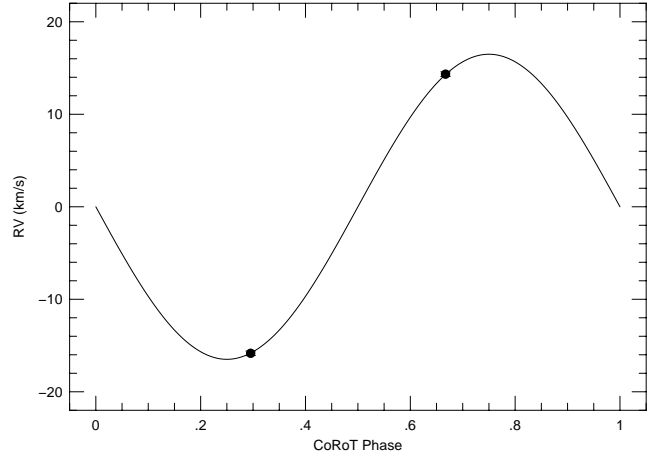
---

[4] We remind the reader that the mass function expressed in solar units is defined as $f(m) = M_2^3\,(sin^3 i)/(M_1 + M_2)^2 = (1.03608 \times 10^{-7})(1 - e^2)^{3/2}\,K_1^3\,P$, where M_1 and M_2 are the masses in solar units of the primary and secondary component, i and e the orbit inclination and eccentricity, K_1 the RV semi-amplitude of the primary star in km s^{-1}, and P the orbital period expressed in days.

components vary in phase with twice the transit period and with a maximum velocity difference of about 67 km s^{-1}. This is a blend scenario: a probable hierarchical triple system consisting of a K5 primary active dwarf orbited by two eclipsing active M-type stars that are too faint to be seen in the metallic lines used for the RV measurements.

6.2.8. LRa01 E2 1145 - CHR - 0102707895

A transit with the following parameters is detected in the *CoRoT* lightcurve: $D = 0.43\%$ and $P = 5.78$ days. The $V = 13.96$ mag target is already known from the *CoRoT* IRa01 run (IRa01 E1 1873; Carpano et al. 2009) and is classified as a A9 IV/V star on the basis of AAOmega observations. SOPHIE measurements spectroscopically resolve the target as a SB1 system with a RV curve in anti-phase with the *CoRoT* ephemeris. Assuming a circular orbit, the RV curve semi-amplitude of the eclipsing star is K=23.5 km s^{-1}.

6.2.9. LRa01 E2 1897 - MON - 0102658070

This $V = 14.72$ mag candidate, classified as a F2 II star according to Exo-Dat, shows a deep transit-like signal ($D = 2.80\%$) with a period of 4.67 days. Hints of a secondary eclipse are detected in the *CoRoT* lightcurve at phase=0.5. CFHT photometric observations show that the signal originates from an eclipsing binary located ∼ 3″ Northeast from the *CoRoT* main target. The contaminant exhibits flux variation of about 7.8% occurring at the predicted *CoRoT* ephemeris. This is consistent with the transit signal when the dilutions by the main target and by a second brighter star located 24.4″ Southwest, are considered. This candidate is a contaminating eclipsing binary (CEB).

6.2.10. LRa01 E2 2249 - CHR - 0102755837

This candidate has a 0.38% deep transit occurring every 27.93 days. Low-resolution spectra obtained with AA0mega classify the star ($V = 13.88$ mag) as K0 III/IV, in good agreement with the Exo-Dat spectral type (K0 III). SOPHIE RV measurements show the candidate to be a SB1 system (K=12 km s^{-1}). Figure 8 shows the RV measurements with a sine fit using the *CoRoT* transit period and epoch. The mass function for the system is $f(m) = 0.0052\ M_\odot$. Assuming a primary mass of $1\ M_\odot$ this results in a secondary mass of $0.17\ M_\odot$.

6.2.11. LRa01 E2 2481 - CHR - 0102723949

The *CoRoT* lightcurve of this candidate ($V = 13.96$ mag, SpT=F5 III; Exo-Dat) contains transits with a depth of 1.20% and a period of 51.76 days. It is also found in the IRa01 run (IRa01 E1 2046) and listed as a mono-transit candidate in the IRa01 report papers (Carpano et al. 2009; Moutou et al. 2009). The spectral classification based on low-resolution spectroscopy performed with AAOmega hints at a stellar binary. According to the method described in Gandolfi et al. (2008), the spectral type of this object "changes" from G0 V to G8 V as a function of the fitted spectral region, suggesting the presence of two stellar objects whose lines are blended in the low-resolution AAOmega spectrum. A single epoch SOPHIE spectrum shows a SB2 system (Moutou et al. 2009), confirming the AAOmega binary scenario.
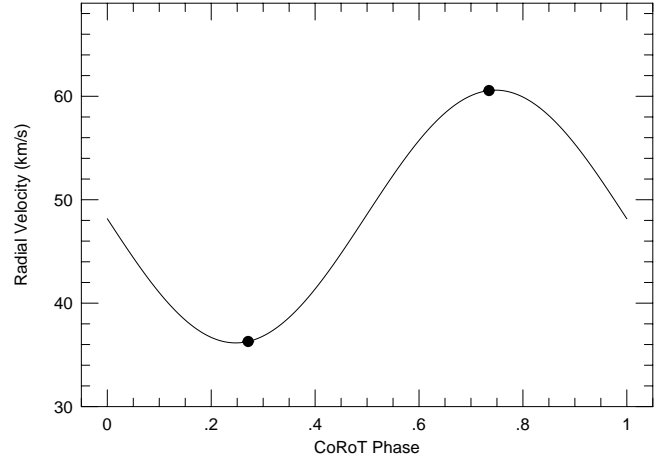
Fig. 8. The SOPHIE RV measurements of LRa01 E2 2249 (points) with a sine-fit (line) using the *CoRoT* transit period and epoch.

6.2.12. LRa01 E2 2694 - CHR - 0102590741

Transit events with 1.30% depth and a 30.40 days period are found in the lightcurve of this star ($V = 13.56$ mag, SpT=A0 IV; Exo-Dat). SOPHIE and HARPS spectra show no CCF and only He I absorption and strong emission Balmer lines, indicative of a Be-type star. Low-resolution AAOmega spectra confirm the SOPHIE results and yield a spectral type of B3Ve which translates into a stellar radius of about 5 $R_\odot$ (Cox 2000). Taking into account the contamination level for this star (∼ 14% according to Exo-Dat), the observed transit, if on target, is therefore caused by a stellar object with a radius of about 0.6 $R_\odot$.

6.2.13. LRa01 E2 4129 - MON - 0102590008

The $V = 15.71$ mag G0 IV target star (Exo-Dat) has two faint nearby contaminants located about 4.5″ to the North-Northeast. Wise observations are inconclusive. EulerCam photometric observations show no signs of transits on the main target. Instead a 7% drop in brightness is found in one of the two contaminant stars which accounts for the transit events observed on LRa01 E2 4129 (0.18% deep eclipses every 1.94 days). Therefore, this case is classified as a contaminating eclipsing binary (CEB).

6.2.14. LRa01 E2 5084 - MON - 0102667981

This $V = 15.95$ mag transit candidate is classified as a A5 subgiant star according to Exo-Dat. The transit is 0.28% deep with a 9.92 days period. Based on HARPS observations, the candidate is a SB1 system. Assuming a circular orbit, the HARPS measurements yield a $K = 37.2$ km s^{-1} RV curve in anti-phase with the *CoRoT* ephemeris.

6.2.15. LRa01 E2 5184 - CHR - 0102779966

This V=15.41 mag candidate ($D = 0.41\%$, $P = 7.37$ days), classified as K2 V star in Exo-Dat, is already known from the IRa01 field as IRa01 E1 4108 Carpano et al. (2009); Moutou et al. (2009). CFHT ground-based photometry confirms the transit to be on target. HARPS spectra yield $T_{\rm eff} = 5000 \pm 100\ K$, $log\ g = 4.4 \pm 0.1$ dex, $[M/H] = 0.07 \pm 0.06$ dex, $v \sin i = 1.5 \pm 0.5$ km s^{-1},

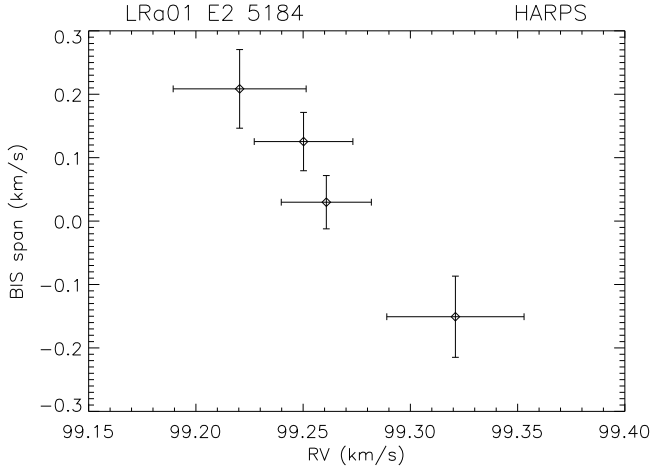**Fig. 9.** CCF bisector spans versus RV measurements as derived from the HARPS spectra of LRa01 E2 5184.

and SpT = K0 V. HARPS data also indicate a strong bisector-RV correlation consistent with a blended eclipsing binary (i.e., diluted triple system or background/foreground eclipsing binary), as shown in Figure 9.

6.2.16. LRa01 E2 5747 - MON - 0102753331

This candidate (V = 16.16 mag) is already known from the IRa01 field as IRa01 E1 4617 (Carpano et al. 2009; Moutou et al. 2009). The transit is 3.64 % deep, appears every 19.75 days, and has a duration of 14.13 hours suggesting a stellar companion. No CCF is detected with HARPS. The spectrum shows only broad Balmer and Mg i-b lines, indicative of a rapidly rotating A-type star, in agreement with the Exo-Dat spectral classification (A5 IV). Even assuming a late A-type dwarf star, the stellar radius would be too large ($R_* > 1.5\ R_\odot$; Cox 2000) to make the observed 3.64 % deep transit of planetary origin. Therefore the transiting object, if on target, is a stellar companion.

6.2.17. LRa01 E2 3739 - MON - 0102755764

The *CoRoT* lightcurve of this candidate (V = 15.55 mag) shows a V-shaped, 2.93 % deep transit signal with a duration of 6.97 hours and a period of 61.48 days, superimposed on a low-amplitude pulsation (Debosscher et al. 2009). Shape, duration, and depth suggest grazing eclipses of an evolved star by a stellar companion. A single transit event was already observed in the IRa01 field (IRa01 E1 4014), whereas two transits are found in the LRa01 lightcurve. EulerCam observations confirm the transit to be on target but 0.14 days after the predicted ephemeris. Taking into account the transit timing error of about 0.07 days at the time of the EulerCam follow-up (25 January 2009), the observed transit occurred only 2σ after the predicted event. Nearby stars were either stable during the observation or their variation was too small to account for the transit signal detected in the *CoRoT* lightcurve. Therefore the transit is concluded to be on target. HARPS observations show no CCF for this target. Only broad Balmer lines are visible in the HARPS spectrum. This is consistent with the star being a rapidly rotating A-type star, in agreement with the Exo-Dat A5 IV spectral type. As described in Section 6.2.16, an eclipsing stellar companion star is suspected
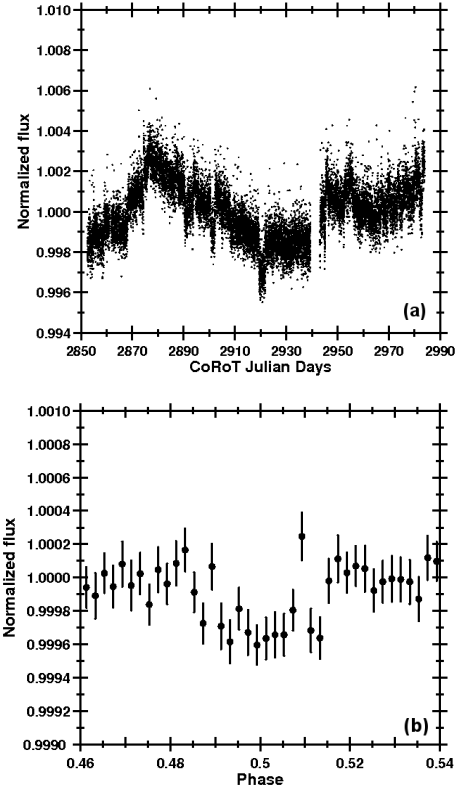
Fig. 10. *Top panel*: Raw white lightcurve of LRa01 E1 0286 which shows instrumental effects (jumps). *Bottom panel*: Normalized and phase-folded white lightcurve of the transit candidate LRa01 E1 0286 at the period P = 3.60 days after filtering with ExoTrans (Grziwa et al. 2011). Additional filtering was necessary to make the transit visible in this example.

to orbit around this candidate and follow-up observations are completed.

6.2.18. LRa01 E2 5756 - MON - 0102582529

A 2.72 % deep transit with a period of 15.84 days is found in the *CoRoT* lightcurve of this V = 16.24 mag candidate, whose spectral type is F0 V according to Exo-Dat. The transit signal is rather deep and the ingress/egress steeper than expected for a planetary candidate. But it is not ruled out as a binary on the photometric level, because the transit can also be produced by a planet with a higher impact parameter.

IAC80 photometry establises that the transit event is on-target. Spectral observations with HARPS reveals no CCF. The spectrum is consistent with LRa01 E2 5756 being a rapidly rotating A-type star. No further follow-up observations are foreseen since the transiting object is suspected to be a stellar companion.

6.3. Unsettled good planetary candidates

6.3.1. LRa01 E1 0286 - CHR - 0102742060

A shallow eclipse (0.03 %) in the lightcurve of this relatively bright star V = 13.30 mag was discovered at a period of 3.60 days (Figure 10).

Initially, this candidate was regarded as a possible 1.9 R_{Earth}-sized planet around a main sequence solar-like star. However, reconnaissance spectroscopy performed with SANDIFORD in
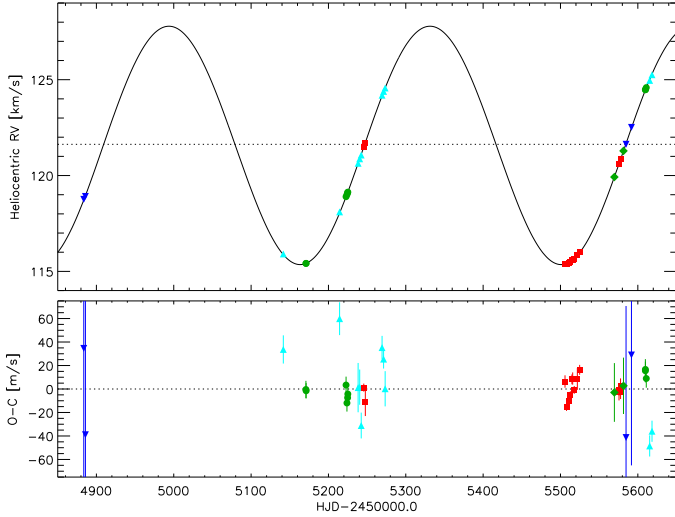
Fig. 11. *Top panel*: RV curve of LRa01 E1 0286 as observed with Sandiford (blue downward triangles), SOPHIE (light blue upward triangles), HIRES (green circles), HARPS (red squares), and FIES (green diamonds). The solid line represents the best fitting Keplerian orbital fit to the data (see text for more details). A RV shift was let free to vary in the fit between the five data-sets. The systemic RV of $V_\gamma = 121.603$ km s^{-1}, as derived from the HARPS data-set only, is plotted with a horizontal dotted line. *Bottom panel*: The RV residuals after subtracting the orbital solution (see the on-line edition of the Journal for a colour version of this figure).

February 2009 suggests that the target is a G8/9 IV star. Additional observations with HIRES and HARPS indicate $T_{\rm eff} = 5250 \pm 80\,K$, $log\,g = 3.75 \pm 0.10$, $[M/H] = -0.10 \pm 0.05$, and $v\sin i = 3.0 \pm 1.0\,{\rm km\,s}^{-1}$, compatible with an evolved star of $M_* \approx 1.1\,M_\odot$ and $R_* \approx 2.3\,R_\odot$. This excluded a terrestrial-sized object but a transiting planet with $R_P \approx 4.4\,R_{Earth}$ was still possible.

RV observations carried-out over two years with SOPHIE, HIRES, HARPS, FIES, and SANDIFORD revealed a long-term RV trend indicative of an SB1 not in phase with the *CoRoT* transit ephemeris. The orbital fit to the data is shown in Fig. 11. The orbit seems nearly circular ($e \approx 0.01$) with a period of $P = 337.52 \pm 0.20$ days and has a RV semi-amplitude $K = 6.22 \pm 0.18\,{\rm km\,s}^{-1}$. The derived mass function $f(m) \approx 0.0084\,M_\odot$ implies a companion mass of approximately $0.22\,M_\odot$ assuming $1.1\,M_\odot$ for the primary star's mass.

The residuals to the binary orbit fit have a rms scatter of about $7.5\,{\rm m\,s}^{-1}$ when using only the higher quality HARPS and HIRES data. Fig. 12 shows the residual RV measurements phased to the *CoRoT* transit period. There is no convincing sinusoidal variations. The RV semi-amplitude of a possible planetary companion orbiting the target star would have to be less than about $5\,{\rm m\,s}^{-1}$.

Recent time-series photometric observations performed with MegaCam@CFHT3.6m and EulerCam@Euler1.2m suggest that a faint, nearby star ($R \approx 18$ mag, 5″ South from the target) might experience eclipses of $\sim 5\,\%$ that would account for the detected $0.03\,\%$ transit-like signal on LRa01 E1 0286. However, the photometric follow-up is still not conclusive and further investigation are needed to assess the real nature of the candidate. In conclusion, the target star is part of a long period binary and the transit signal remains unresolved. The LRa01 E1 0286 candidate
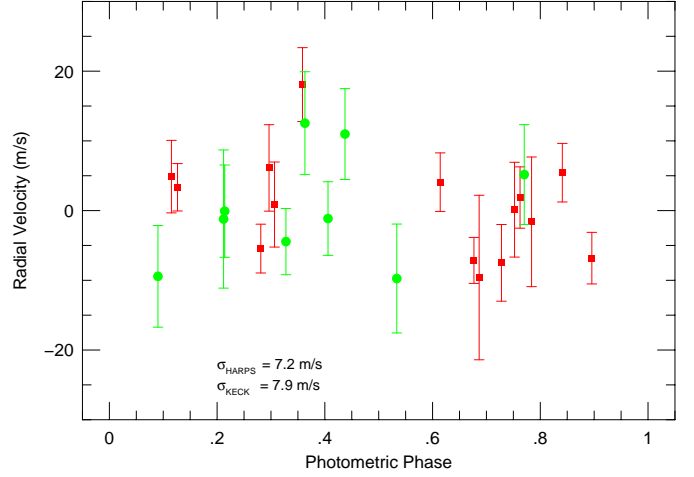
Fig. 12. The HARPS (red squares) and HIRES (green circles) RV residuals of LRa01 E1 0286 phased to the *CoRoT* transit period P=3.60 days and epoch. The root main squares to the binary orbit fit, when considering only the HARPS and HIRES data, are reported in the labels (see the on-line edition of the Journal for a colour version of this figure).

might be either a planet in a stellar binary system or a contaminating eclipsing binary.

6.3.2. LRa01 E1 2101 - CHR - 0102568803

According to Exo-Dat, this $V = 14.15$ mag target is of spectral type K1 III. The *CoRoT* lightcurve shows a 2 % sun-spot-induced variability with a period of ∼11 days. LRa01 E1 2101 appears to be orbited by a transiting object ($D = 0.08\,\%$, $P = 2.72$ days). The signal is only significant in the red *CoRoT* photometric channel. As already described in Section 3, due to the star's PSF on the CCD and the choice of the photometric mask, the expected depth of the transit in the green and blue *CoRoT* photometric channels is smaller than the scatter of the data-points, preventing any comparison of the transit depth in the different channels. Therefore, it cannot be concluded from *CoRoT* data alone that the candidate is a contaminating eclipsing binary. The fist HARPS spectrum reveals a narrow single peak CCF (FWHM=8 km s^{-1}) and a K6 V star with $T_{\rm eff} \approx 4250$ K and $log\,g \approx 4.5$ dex ($M_* \approx 0.7\,M_\odot$, $R_* \approx 0.7\,R_\odot$). The shallow transit depth thus implies a companion radius of about $2\,R_\oplus$. But the transit is V-shaped suggesting a grazing transit/eclipse. Combined measurements with CFHT and MONET-North exclude background eclipsing binaries. The transit is considered to be on target. Six RV measurements acquired with HARPS show no significant sinusoidal variation down to a precision of 18 m s^{-1}. Follow-up is ongoing.

6.3.3. LRa01 E1 2240 - CHR - 0102698887

The transit signal occurs every 2.03 days in the lightcurve of this $V = 15.22$ mag target, classified as a F8 sub-giant according to Exo-Dat. The shallow (0.09 % deep) signal is a little asymmetric when phase-folded. However, due to the low S/N ratio, the transit shape cannot be used to rule out a no-planet scenario. If the candidate is a planet, the transit depth suggests a Neptune-like planetary radius. No follow-up observations have been made yet.

6.3.4. LRa01 E1 3216 - MON - 0102754163

This is a faint $V = 15.7$ mag A5 IV candidate (Exo-Dat) with a periodic 3.11 days transit signal of depth 0.13 %. It shows shallow out of transit variations. No ground-based follow-ups have been performed yet.

6.3.5. LRa01 E1 3221 - MON - 0102634864

This is a rather long-period candidate with $P = 32.33$ days. The transit is V-shaped and 2.33 % deep. This target of brightness $V = 15.58$ mag is listed in Exo-Dat as a A5 dwarf star. However, pulsations with periods of 0.78 and 8.75 days typical for giant stars have been detected in the *CoRoT* lightcurve, in disagreement with the main sequence scenario. No follow-up observations have been made.

6.3.6. LRa01 E1 4423 - MON - 0102782651

A faint ($V = 16.22$ mag) candidate showing a V-shaped shallow transit ($D = 0.25$ %) with a period of 1.87 days. No follow-up observations have been carried out. The *CoRoT* lightcurve is strongly affected by instrumental effects (jumps). Exo-Dat list the spectral type as K4 V.

6.3.7. LRa01 E1 4594 - MON - 0102617334

This transiting candidate ($D = 0.27$ %) was not spectroscopically observed due to the faintness of the target star ($V = 16.66$ mag, SpT =O8 III from Exo-Dat). IAC80 photometry excludes background eclipsing binaries. The transit duration of 6.6 hours for a transit period of $P = 5.49$ days is consistent with an evolved host star.

6.3.8. LRa01 E1 4667 - MON - 0102588881

A 1.52 % deep transit signal with a period of 27.29 days is found in the lightcurve of this $V = 16.08$ mag star of spectral type A5 IV (Exo-Dat). Wise photometric observations are inconclusive due to bad weather. IAC80 observations exclude contaminating eclipsing binaries. Two RV measurements acquired with HARPS at photometric phases 0.43 and 0.76 shows a radial velocity variation of 84 m s^{-1} which is comparable to the errors (i.e., ~70 m s^{-1}). The HARPS spectra unveils a G0 V star, in disagreement with Exo-Dat. Assuming $M_* = 1\,M_\odot$ for the host-star, a Jupiter-mass planet in a 27.29 days orbit around LRa01 E1 4667 would produce a peak-to-peak RV variation of $\approx$ 120 m s^{-1} which is almost twice the HARPS errors. Although the RVs exclude a stellar/brown dwarf companion to LRa01 E1 4667, considerably more HARPS measurements are required to assess the real nature of the transiting object. Follow-up is ongoing.

6.3.9. LRa01 E1 4719 - MON - 0102703155

A 1.26 days period transit signal of depth 0.10 % is found in the *CoRoT* light curve of this $V = 15.88$ mag candidate (SpT=F8 IV, Exo-Dat). The transit is V-shaped and asymmetric when phase-folded. However, the S/N ratio of the detected events is low. The shape may be distorted by either stellar activity or photometric noise. EulerCam could not observe the transit on target. This is expected given the shallow transit depth. Although the transit timing error at the time of the EulerCam observations (28

October 2010) was ±2 hours and there is a risk that the transit might have been missed, it is concluded from photometric on-off observations that large variations by contaminants are probably not the cause for the transit event. No RV-measurements, however, have been acquired.

6.3.10. LRa01 E1 4820 - MON - 0102751316

This is a transiting candidate with a depth of 0.46 % and a period of 1.61 days. Photometric follow-up with the ESA-OGS facility confirms that the transit is on target. Analysis of the lightcurve indicates possible depth differences between odd and even transits and out-of-transit variation. The A5 IV star (Exo-Dat) is too faint ($V = 16.15$ mag) for RV confirmation.

6.3.11. LRa01 E1 5320 - MON - 0102666452

This is another transiting candidate around a faint star ($V = 16.13$ mag, SpT=G2 V; Exo-Dat). The 0.14 % deep signal can only be identified when phase-folded with a 1.97 days period. The 3.3 hours transit duration appears to be a little long for a planetary object. No ground-based observations have been made.

6.3.12. LRa01 E1 5536 - MON - 0102670085

The *CoRoT* lightcurve of this $V = 16.21$ mag star of spectral type F8 IV (Exo-Dat), shows a 0.27 % deep transit signal occurring every 0.90 days. CFHT photometric observations find a 0.40 ± 0.25 % deep transit on target, compatible with the *CoRoT* signal. However some background stars, spatially located around the target, cannot be excluded as possible contaminants and the observations are considered inconclusive. No spectroscopic data have been acquired.

6.3.13. LRa01 E2 3156 - CHR - 0102716818

The target ($V = 15.76$ mag) is a K2 III star according to Exo-Dat. The 0.15 % deep transit signal appears every 1.47 days and is detected only in the red *CoRoT* channel. As for LRa01 E1 2101 candidate (Section 6.3.2), also in this case the photo-noise in the green and blue channels is larger than the expected depth. The transit is V-shaped, and the duration of 2 hours is quite long for a planet. Observations with IAC80 exclude contamination by neighbouring objects. The transit is likely on target with a 20-30 % chance of a missed transit due to timing error. Two and seven RV measurements with HARPS and HIRES, respectively, show no significant variations down to a precision of 10 m s^{-1}. The candidate is still under investigation.

6.3.14. LRa01 E2 3619 - MON - 0102765275

V-shaped transit signals of 6 % depth with a period of 50.91 days are found in the lightcurve of this star ($V = 15.56$ mag). The spectral type is G8 V, according to Exo-Dat. Low-resolution spectroscopy performed with AAOmega indicates that the target is a G0 IV/V star. However the *CoRoT* photometric data show multi-periodic variations that seem more consistent with a giant. Therefore, the true spectral type is unclear. This candidate is also found in the IRa01 field (as IRa01 E1 2060; Carpano et al. 2009).

6.3.15. LRa01 E2 4519 - MON - 0102580137

A 0.14 % deep candidate with a period of 2.37 days is detected in the lightcurve of this A5 IV star (Exo-Dat) candidate with magnitude $V = 15.75$ mag. EulerCam and IAC80 find no relevant photometric variations in any of the nearby stars. However, the transit may have been missed due to large (1.5 hours) timing errors. Still, the transit is considered to be likely on target. No RV measurements have been acquired for this star.

6.4. Unsettled low priority planetary candidates

Many likely binary candidates are discovered at the photometric level and have a low priority in the follow-up observation chain. Consequently, many of these were not observed by the follow-up team, especially when the target star is faint.

6.4.1. LRa01 E1 2970 - CHR - 0102625386

The $V = 14.49$ mag candidate shows a V-shaped, 0.62 % deep transit signal occurring every 34.10 days. The transit is only seen in the *CoRoT* red channel. No event is detected in the blue and green channels at 4 and 5 σ significance, respectively. This is a characteristic sign of a contaminant eclipsing binary. Hints of secondary eclipse are also detected in the red lightcurve. Exo-Dat lists the spectral type as A5 IV. No follow-up observations have been performed for this star as the candidate is suspected to be a contaminating eclipsing binary (CEB).

6.4.2. LRa01 E1 3617 - MON - 0102617210

According to Exo-Dat this is a A0 V star ($V = 15.62$ mag). The 0.64 % deep signal has a period of 2.73 days. Several coherent frequencies are found which hint to stellar variability induced by a massive companion. Hints of a secondary shallow eclipse have been recently found in the *CoRoT* lightcurve. No follow-up observations were carried out as a binary system is suspected for this candidate.

6.4.3. LRa01 E1 3674 - CHR - 0102732757

A V-shaped transit signal is found in the lightcurve of this A0 V star ($V = 15.32$ mag, Exo-Dat). The transit duration of 3.38 hours is quite long for a 1.97 days transit period. The 0.20 % deep signal can only be seen in the red *CoRoT* channel. It is not detected, neither in the green nor in the blue channel, with a ~3 σ significance. No follow-up observations have been performed on this candidate as a CEB scenario is suspected.

6.4.4. LRa01 E1 4272 - MON - 0102626872

The detected transit of this object is 2.44 % deep with a 1.88 days period. In Exo-Dat the star is listed as A0 V with a brightness of $V = 15.87$ mag. Photometry with ESA-OGS shows the transit to be on target. Due to out-of-transit variations in the lightcurve a stellar binary is suspected.

6.4.5. LRa01 E1 4777 - CHR - 0102620061

A V-shaped transit signal with a period of 3.35 days and a depth of 1.96 % is detected in the lightcurve of this $V = 15.26$ mag candidate (A5 IV, Exo-Dat). The duration (3.90 hours) is rather long for a V-shaped transit and the depths observed in the three

CoRoT colors differ by more than 1 σ. IAC80 observations performed in February 2011 shows no variations neither on target nor on any of the nearby stars. An underestimate of the transit timing error, listed at about 30 minutes at the time of the IAC80 observations, might account for the no ground-based transit detection. No RV follow-up observations have been carried out for this candidate.

6.4.6. LRa01 E1 4836 - MON - 0102630623

Analysis of this V-shaped transit candidate ($D = 4.70$ %, $P = 36.78$ days) shows significant depth difference between even and odd transits (12σ). It is therefore a low priority candidate for which no follow-up observations have been carried out. Exo-Dat lists the spectral type of this $V = 15.85$ mag star as A5 V.

6.4.7. LRa01 E1 5450 - MON - 0102595916

The 0.22 % deep transit signal in the lightcurve of a G0 IV star of brightness $V = 16.38$ mag (Exo-Dat) appears to have an asymmetric shape. In addition, the transit duration of 9.23 hours is too long for the 4.11 days transit period to be consistent with a planet. Due to the faintness of the star and the bad transit properties the candidate has a low priority in the follow-up chain and was not observed.

6.4.8. LRa01 E2 2185 - MON - 0102729260

A G2 V star with $V = 15.08$ mag (Exo-Dat) shows V-shaped transit signals with a depth of 0.24 % and a period of 1.69 days. The candidate is already known from the *CoRoT* IRa01 run as IRa01 E1 1319 (Carpano et al. 2009). The transit duration of 3.57 hours seems to be quite long for a planetary object. In addition, a secondary eclipse at phase=0.5 and depth differences between even and odd transits were detected. This is most likely a binary system. Follow-up observations for this candidate are not foreseen.

6.4.9. LRa01 E2 2597 - CHR - 0102672065

A 8.90 days transit signal is found in the lightcurve of this $V = 14.17$ mag star. AAOmega spectroscopy shows the candidate to be a G6 III/IV star, in good agreement with the Exo-Dat classification (G5 III). FLAMES yields $T_{\mathrm{eff}} = 4991 \pm 140$ K, $log\, g = 3.24 \pm 0.30$ dex, $[m/H] = -0.29 \pm 0.15$ dex, and $v \sin i = 4.8 \pm 2.0$ km s^{-1} (Gazzano et al. 2009). As described in Section 3, the deep signal (1.00 % when normalized to the blue flux only) is seen only in the *CoRoT* blue channel (Figure 4). The event is detected, neither in the green nor in the red lightcurve, with a 12σ and 25σ significance, respectively. This indicates that the candidate is with high probability a contaminating eclipsing binary (CEB).

6.4.10. LRa01 E2 2627 - CHR - 0102757559

According to low-resolution spectroscopy performed with AAOmega the spectral type of this $V = 15.13$ mag star is F4 V, whereas Exo-Dat lists this target as a G2 V object. A V-shaped deep signal (0.083 %) is found only in the *CoRoT* blue channel, with a significant not-detection in the green and red lightcurves (4σ). This indicates a contaminating eclipsing binary with a period of 0.95 days. Neither photometric nor further spectroscopic follow-up is foreseen.

6.4.11. LRa01 E2 3157 - CHR - 0102672700

The object is a low priority 0.24 % deep candidate (P = 1.87 days) due to 1) V-shaped transit curve, 2) differences in the transit depths at a 5σ significance, and 3) the transit is only seen in the red channel with a $\sim 3\sigma$ significant no-detection in the blue and green colors, suggesting the presence a nearby contaminating eclipsing binary. Exo-Dat lists the spectral type of this V = 14.86 mag star as G0 IV. No follow-up observations have been carried out for this star as a CEB scenario is suspected.

6.4.12. LRa01 E2 4494 - MON - 0102587927

A shallow transit (0.13 %) signal with a period of about 2 days) is found in the *CoRoT* lightcurve of this faint (V = 16.07 mag) target. Exo-Dat list the spectral type as K3 V. The apparent transit shape is asymmetric and the transit duration (2.81 hours) is quite long for the orbital period. No follow-up observations have been performed on this candidate.

6.4.13. LRa01 E2 4910 - MON - 0102780627

This is a candidate around a star of brightness V = 15.36 mag listed as a F8 dwarf in Exo-Dat. It has been also detected in the IRa01 run (IRa01 E1 1531) and listed as a planetary candidate in Carpano et al. (2009). Observations with AAOmega classify this candidate as a F7/8 dwarf star, in really good agreement with Exo-Dat. The transit is 0.87 % deep and appears every 2.38 days. IAC80 observations confirms the transit signal is on target. Due to secondary faint eclipses at phase 0.5 recently detected in the lightcurve, it is suspected to be a binary. No further follow-up is foreseen.

6.4.14. LRa01 E2 5194 - MON - 0102604000

This candidate is suspected to be a binary. The 2.8 hours duration of the 0.68 % deep transit is too long for a transiting planet with an orbit period of 1.25 days around a K2V star (Exo-Dat). No spectroscopic follow-up observations have been made due to the faintness of the star (V = 16.09 mag) and the lack of ground-based confirmation that the transit is on-target.

6.5. False alarms

Sometimes, *CoRoT* lightcurves are affected by instrumental effects (e.g., jumps, glitches) making the transit detection uncertain.

6.5.1. LRa01 E1 2960 - CHR - 0102613782

There appears to be a 0.17 % deep transit with a 13.03 days period in this lightcurve of a V = 14.40 mag F8 IV star (Exo-Dat). This signal can only be found in the *CoRoT* red channel which is affected by instrumental effects (jumps). If real and on target the transit should be visible in the green and blue channel as well. Therefore, it is suspected to be a false alarm.

6.5.2. LRa01 E2 3389 - CHR - 0102674894

This shallow transit signal (D = 0.08 %, P = 7.03 days) is found in the lightcurve of a faint (V = 15.65 mag) G0 III star (Exo-Dat), but the lightcurve is disturbed by instrumental effects (jumps). It is suspected to be a false alarm.

6.5.3. LRa01 E2 3612 - MON - 0102577194

A 0.34 % deep transit signal with a period of 38.24 days is found in the lightcurve of this faint object (V = 16.01 mag), listed as a G0 IV star in Exo-Dat. The shape of the transit is asymmetric and the data suffer from glitches and jumps. This is likely a false alarm.

6.6. X-cases

The following stars are objects that might be planetary candidates if the spectral type of the target was considerable different than listed in Exo-Dat.

6.6.1. LRa01 E2 0928 - MON - 0102664130

The target star of this 2.60 % deep transit candidate is according to Exo-Dat a A5 IV star, implying a stellar radius of about 2 $R_\odot$ (Cox 2000). If true, the V-shaped signal, occurring every 49.9 days, cannot be caused by a planet. But the true spectral type of a star can differ significantly from the one given in Exo-Dat. Therefore the candidate was not completely discarded as a binary pending the confirmation of the spectral type. Unfortunately, the star is very faint (V = 15.62 mag) making a rapid spectral type classification difficult.

6.6.2. LRa01 E2 5678 - MON - 0102613411

Another deep candidate which might be a planetary candidate if the true stellar radius is smaller than listed in Exo-Dat (i.e., $R_* \approx 1.1 R_\odot$ for a F8 V star). The transit is 4.33 % deep and occurs every 18.76 days. Unfortunately, the star is relatively faint (V = 15.91 mag) making it a difficult target for a rapid spectral type classification.

6.7. Mono-transits

6.7.1. LRa01 E1 2765 - MON - 0102647266

A mono-transit candidate is found with D = 8.30 % at epoch HJD = 2454465.434 in the light curve of a A5 V star of magnitude V = 14.52 mag (Exo-Dat).

6.7.2. LRa01 E1 4785 - CHR - 0102709133

This single transit (D = 9.70 % at HJD = 2454419.798) is more prominent in the blue channel and there might be a secondary smaller eclipse at HJD = 2454524.348 with a depth of $\sim$ 1 %. This candidate is probably a contaminating eclipsing binary with a period of $\sim$ 209 days. The target star is listed in Exo-Dat as a K2 V star with magnitude V = 15.50 mag.

6.7.3. LRa01 E2 1113 - CHR - 0102574444

At epoch HJD = 2454422.342 a 5.40 % deep transit can be found in the lightcurve of this star. The transit signal is deeper in the blue channel. Probably the transiting object does not orbit this F8 IV star of brightness V = 14.14 mag (Exo-Dat). It is a suspected contaminating eclipsing binary.
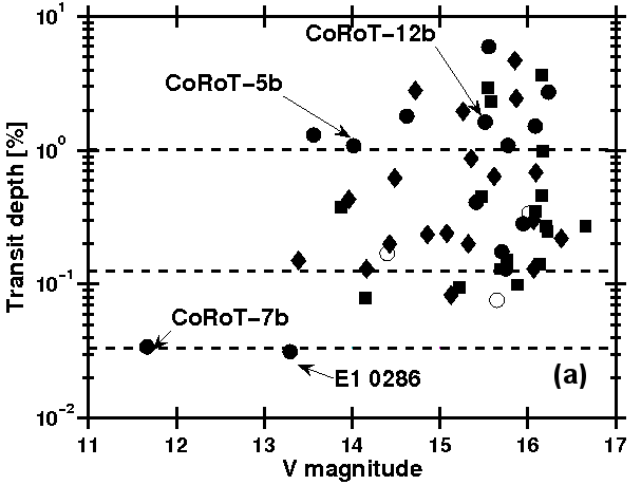
Fig. 13. Transit depth (D) versus V magnitude of the candidates found in LRa01 by the detection group after exploiting the full length of the lightcurves. Filled circles are good planetary candidates, squares are low priority candidates, diamonds are suspected binaries, and open circles are suspected false alarms. Arrows mark the three transiting planets found in the LRa01 run: CoRoT-5b, CoRoT-7b and CoRoT-12b, and the suspected planet LRa01 E1 0286. The horizontal dashed lines represent (from top to bottom) the expected signal produced by a Jupiter-size planet, a Neptune-size planet and a 2 Earth radii planet around a solar-like star, respectively.

6.7.4. LRa01 E2 2368 - MON - 0102582649

A single very deep transit/eclipse ($D = 17.80\%$) is found at epoch 2454510.992 HJD. The $V = 14.98$ mag object is listed in Exo-Dat as F6 V star.

6.7.5. LRa01 E2 2744 - MON - 0102586624

At epoch $HJD = 2454473.174$ a 15.75 % deep single transit/eclipse is visible in the lightcurve of this object. The star is listed in Exo-Dat as A5 IV and magnitude $V = 15.11$ mag.

7. Discussion

CoRoT-7b (Léger et al. 2009) and the candidate LRa01 E1 0286 proves the capability of CoRoT for discovering Super-Earths around main-sequence stars. Although the latter candidate is maybe not a Super-Earth, the depth of the detected transit is comparable to the signal expected from a *bona fide* Super-Earth around a solar-like star. Therefore, it is concluded from Figure 13 that CoRoT is capable of detecting Super-Earths with periods in the range of one to four days around stars of apparent magnitude $V \leq 13.3$ mag. However, most of the target stars are fainter than this limit (Figure 1). The CoRoT-7b case was favourable for the terrestrial-size planet detection. Indeed the planet orbits a star of magnitude $V = 11.65$ mag in less than one day. CoRoT-7 is one of the brightest objects in the LRa01 star field. The follow-up for the candidate LRa01 E1 0286 proved to be much more difficult although the star of magnitude $V = 13.30$ mag is still quite bright compared to others in the field.
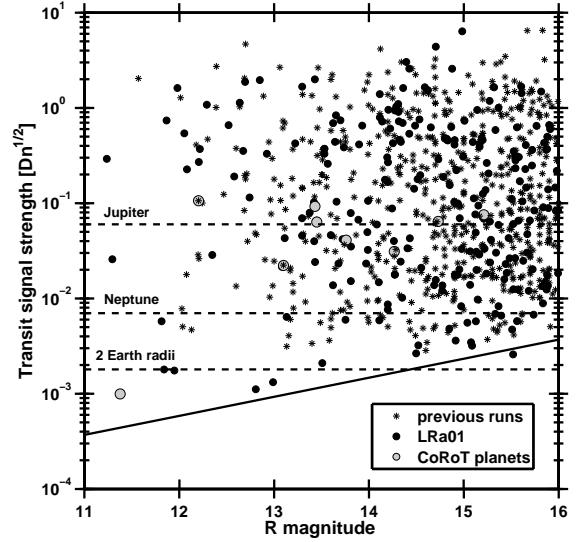
Fig. 14. Transit signal strength versus r' magnitude of detected planetary and binary candidates for the previous IRa01, SRc01, LRc01 CoRoT runs (asterisks), LRa01 run (filled circles), and first seven CoRoT-planets (open circles). D is the transit depth and n is the number of points in a transit event. The horizontal dashed lines represent (from top to bottom) the expected signal produced by a Jupiter-size planet, a Neptune-size planet, and a 2-Earth radii planet around a solar-like star, respectively. Transit candidates and binaries have been combined in this example to have a better statistical basis of the detection efficiency. The solid line represents the photon noise.

Compared to previous CoRoT runs (i.e., IRa01, SRc01, and LRc01) more and weaker candidates have been found in the LRa01 field (Figure 14 and 15). This is to be expected, since LRa01 covers a longer time period than SRc01 and IRa01 (≈ 25 days for SRc01 and ≈ 90 days for IRa01). The lack of small transit candidates around bright stars in the LRc01 star field is explained by the unfavourable stellar population properties of this particular star field for the search of extrasolar planets: 58 % of all stars were identified as giants. Furthermore, LRc01 contains in total less stars with apparent magnitude $V < 13$ mag. On the other hand, the LRa01 star field contains at least 62 % main sequence stars. Overall, it contains more bright main sequence stars with apparent magnitude $V < 13$ mag than previous long runs (Section 2 and Table 3). Planets around such stars are easier to detect in the photometric data and easier to observe by ground-based telescopes. From the perspective of the types of false positives and *bona fide* transiting planets identified in LRa01 with respect to IRa01 and LRc01, we found that the rates of discovered planets, spectroscopically confirmed eclipsing binary systems, CEB, and blends is comparable between the three runs.

The lack of confirmed Neptune-size planets is probably not due to limitations in the CoRoT follow-up or detection chain. Although the follow-up is constrained by the limited observation time as pointed out by Moutou et al. (2009), CoRoT was able to find at least one Super-Earth and other planet search programs yield similar result. Short-period Neptune-size planets may be very rare objects, as tentatively pointed out 2005 by Mazeh et al. (2005) and as seems to be confirmed by the distribution of Kepler planetary candidates (Borucki et al. 2011).

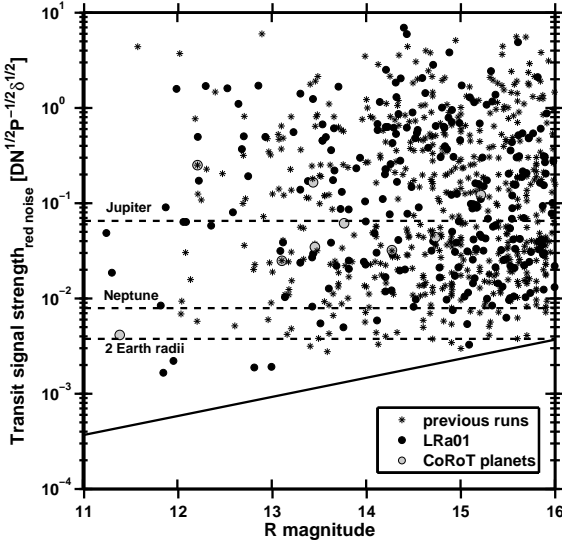**Fig. 15.** Transit signal strength in the presence of red noise versus r' magnitude for the detected and binaries candidates in the previous IRa01, SRc01, LRc01 *CoRoT* runs (asterisks), LRa01 run (filled circles), and the first seven *CoRoT*-planets (open circles). D is the transit depth, N is the number of data points in a lightcurve, P is the transit period, and $\delta = 512$ seconds is the sampling interval. The horizontal dashed lines represent (from top to bottom) the expected signal produced by a Jupiter-size planet with 3 days orbit period, a Neptune-size planet with 3 days orbit period and a 2 Earth radii planet with 1 day orbit period around a solar-like star, respectively. The solid line represents the photon noise.

Table 3. Number of bright main sequence stars in LRa01 and the previous runs.

CoRoT run	Number of dwarf stars with $V < 13$ mag
IRa01	308
LRc01	138
LRa01	438

Such planets may evaporate faster than more massive gas giants because their low surface gravity is not able to maintain the irradiated atmosphere (Southworth et al. 2007). Davis & Wheatley (2009) provide further evidence for a lost population of short-period Neptune planets. Almenara et al. (2009), after analysis of three *CoRoT* fields, further support the conclusion that the lack of confirmed Neptune planets in the *CoRoT* fields is not due to observational limitations.

8. Summary

CoRoT observed the LRa01 star field continuously for 130 days and collected 11 408 lightcurves. There are 7 470 chromatic photometric data-sets and 3 938 monochromatic data-sets. The *CoRoT* detection group performed a full in-depth analysis of the lightcurves. 242 lightcurves (2.1 % of all lightcurves) contain a transit signal. 191 of these (79 % of the candidates or 1.7 % of all stars in the field) were identified as binaries based on photometric analysis only (Table 7), including five mono-transits (Section 6.7).

Fifty-one signals were classified as planetary candidates and proposed for observational follow-up with different priorities based on the photometric analysis. Thus in about 0.5 % of all *CoRoT* targets a signal was detected that might originate from a planetary transit. In addition, 3 candidates were discarded as likely false alarms based on photometric analysis (Section 6.5). Five mono-transits were detected with depths compatible with an eclipsing binary (Section 6.7 and Table 7). Two candidates were classified as potential planetary candidates or "X-cases" (Section 6.6), if the stellar radius of the target star is significantly smaller than listed in the Exo-Dat database. None of the false candidates and X-cases were followed-up and are included for completeness. See also Table 5.

Of the fifty-one candidates, thirty-seven (73 % of all candidates) are "good" planetary candidates based on photometric analysis only (Sections 6.1, 6.2, and 6.3). Thirty-two of the "good" candidates have been followed-up and the nature of twenty-two objects has been solved. Four candidates (about 8 % of all candidates) have been confirmed as transiting planets (Table 2): *CoRoT*-7b (Léger et al. 2009), *CoRoT*-5b (Rauer et al. 2009), *CoRoT*-12b (Gillon et al. 2010), and the recently confirmed hot-Jupiter LRa01 E2 5277 (*CoRoT*-21b, Pätzold et al. 2011). Another two non-transiting planets were detected by RV measurements only: *CoRoT*-7c (Queloz et al. 2009) and *CoRoT*-7d (Hatzes et al. 2010). Another candidate, LRa01 E1 0286 may be a planetary object in a binary system but is unconfirmed yet. Eighteen objects (49 % of the good candidates) were identified as non-planetary objects. Six are contaminating eclipsing binaries (CEBs) and two are blends (i.e., LRa01 E1,1123 and LRa01 E2 5184). Six candidates could be resolved spectroscopically as stellar binaries (SB). Four candidates are stellar companions around early-type stars.

According to the lightcurve analysis only, fourteen candidates (27 % of all candidates; Section 6.4) have low priorities because of one or more characteristics hinting at a non-planetary scenario: out of transit variations, depth differences between even and odd transits, depth differences in different color channels, and very shallow secondary eclipse. Four of these were followed-up but the observations are not conclusive.

The follow-up for most of the LRa01 candidates is now concluded. Only LRa01 E1 0286, LRa01 E1 2101, LRa01 E1 4667, and LRa01 E2 3156 are still under investigation.

PNP.08A.MOUT, PNP.09A.MOUT, and PNP.10A.MOUT; *c)* the FIES spectrograph at the Nordic Optical Telescope (observing program P42-261), operated on the island of La Palma jointly by Denmark, Finland, Iceland, Norway, and Sweden, in the Spanish Observatorio del Roque de los Muchachos of the Instituto de Astrofisica de Canarias; *d)* the AAOmega multi-object facilities at the Anglo-Australian Telescope operated at Siding Spring Observatory by the Anglo-Australian Observatory (observing programs 07B/040 and 08B/003); *e)* the SANDIFORD spectrograph at the 2.1 m Otto Struve telescope at McDonald Observatory of the University of Texas at Austin; *f)* the MOnitoring NEtwork of Telescopes (MONET), funded by the "Astronomie & Interne" program of the Alfried Krupp von Bohlen und Halbach Foundation, Essen, and operated by the Georg-August-Universität Göttingen, the McDonald Observatory of the University of Texas at Austin, and the South African Astronomical Observatory.

The CoRoT/Exoplanet catalogue (Exo-Dat) was made possible by observations collected for years at the Isaac Newton Telescope (INT), operated on the island of La Palma by the Isaac Newton group in the Spanish Observatorio del Roque de Los Muchachos of the Instituto de Astrofísica de Canarias.

References

Alapini, A. & Aigrain, S. 2008, in IAU Symposium, Vol. 249, IAU Symposium, ed. Y.-S. Sun, S. Ferraz-Mello, & J.-L. Zhou, 89–92

Almenara, J. M., Deeg, H. J., Aigrain, S., et al. 2009, A&A, 506, 337

Alonso, R., Deeg, H. J., Brown, T. M., & Belmonte, J. A. 2004, Astronomical Notes, 325, 594

Auvergne, M., Bodin, P., Boisnard, L., et al. 2009, A&A, 506, 411

Batalha, N. M., Borucki, W. J., Bryson, S. T., et al. 2011, ApJ, 729, 27

Boisse, I., Bouchy, F., Hebrard, G., et al. 2011, A&A, 528, A4

Bordé, P., Fressin, F., Ollivier, M., Léger, A., & Rouan, D. 2007, in Astronomical Society of the Pacific Conference Series, Vol. 366, Transiting Extrapolar Planets Workshop, ed. C. Afonso, D. Weldrake, & T. Henning, 145

Borucki, W. J., Koch, D. G., Basri, G., et al. 2011, ApJ, 736, 19

Brown, T. M. 2003, ApJ, 593, L125

Bruntt, H., Deleuil, M., Fridlund, M., et al. 2010, A&A, 519, A51

Cabrera, J., Fridlund, M., Ollivier, M., et al. 2009, A&A, 506, 501

Carpano, S., Cabrera, J., Alonso, R., et al. 2009, A&A, 506, 491

Carpano, S. & Fridlund, M. 2008, A&A, 485, 607

Cox, A. N. 2000, Allen's astrophysical quantities, ed. Cox, A. N. (New York: AIP Press; Springer)

Cutri, R. M., Skrutskie, M. F., van Dyk, S., et al. 2003, 2MASS All Sky Catalog of point sources, ed. Cutri et al. (NASA/IPAC Infrared Science Archive)

Davis, T. A. & Wheatley, P. J. 2009, MNRAS, 396, 1012

Debosscher, J., Sarro, L. M., López, M., et al. 2009, A&A, 506, 519

Deeg, H. J., Gillon, M., Shporer, A., et al. 2009, A&A, 506, 343

Deleuil, M., Deeg, H. J., Alonso, R., et al. 2008, A&A, 491, 889

Deleuil, M., Meunier, J. C., Moutou, C., et al. 2009, AJ, 138, 649

Deleuil, M., Moutou, C., Deeg, H. J., et al. 2006, in ESA Special Publication, Vol. 1306, ESA Special Publication, ed. M. Fridlund, A. Baglin, J. Lochard, & L. Conroy, 341

Drummond, R., Lapeyrere, V., Auvergne, M., et al. 2008, A&A, 487, 1209

Ferraz-Mello, S., Tadeu dos Santos, M., Beauge, C., Michtchenko, T. A., & Rodriguez, A. 2011, A&A, 531, A161

Gandolfi, D., Alcalá, J. M., Leccia, S., et al. 2008, ApJ, 687, 1303

Gandolfi, D., Hébrard, G., Alonso, R., et al. 2010, A&A, 524, A55

Gazzano, J., Deleuil, M., De Laverny, P., et al. 2009, in IAU Symposium, Vol. 253, IAU Symposium, 404–405

Gillon, M., Hatzes, A., Csizmadia, S., et al. 2010, A&A, 520, A97

Gondoin, P., Fridlund, M., Goupil, M. J., et al. 2009, in American Institute of Physics Conference Series, Vol. 1094, American Institute of Physics Conference Series, ed. E. Stempels, 864–867

Grziwa, S., Carone, L., & Pätzold, M. 2011, MNRAS, tbd, tbd

Hatzes, A. P., Dvorak, R., Wuchterl, G., et al. 2010, A&A, 520, A93

Hatzes, A. P., Fridlund, M., & et al. 2011, ApJ, In preparation

Hekker, S., Kallinger, T., Baudin, F., et al. 2009, A&A, 506, 465

Kabath, P., Eigmüller, P., Erikson, A., et al. 2008, AJ, 136, 654

Klement, R. J., Bailer-Jones, C. A. L., Fuchs, B., Rix, H.-W., & Smith, K. W. 2011, ApJ, 726, 103

Léger, A., Rouan, D., Schneider, J., et al. 2009, A&A, 506, 287

Llebaria, A. & Guterman, P. 2006, in ESA Special Publication, Vol. 1306, ESA Special Publication, ed. M. Fridlund, A. Baglin, J. Lochard, & L. Conroy, 293

Loeillet, B., Shporer, A., Bouchy, F., et al. 2008, A&A, 481, 529

Mazeh, T., Zucker, S., & Pont, F. 2005, MNRAS, 356, 955

Meunier, J.-C., Deleuil, M., Moutou, C., et al. 2007, in Astronomical Society of the Pacific Conference Series, Vol. 376, Astronomical Data Analysis Software and Systems XVI, ed. R. A. Shaw, F. Hill, & D. J. Bell, 339

Michel, E., Baglin, A., Weiss, W. W., et al. 2008, Communications in Asteroseismology, 156, 73

Moutou, C., Aigrain, S., Almenara, J., et al. 2007, in Astronomical Society of the Pacific Conference Series, Vol. 366, Transiting Extrapolar Planets Workshop, ed. C. Afonso, D. Weldrake, & T. Henning, 127

Moutou, C., Pont, F., Barge, P., et al. 2005, A&A, 437, 355

Moutou, C., Pont, F., Bouchy, F., et al. 2009, A&A, 506, 321

Pätzold, M., Endl, M., Csizmadia, S., et al. 2011, A&A, in preparation

Pinheiro da Silva, L., Rolland, G., Lapeyrere, V., & Auvergne, M. 2008, MNRAS, 384, 1337

Pont, F., Aigrain, S., & Zucker, S. 2011, MNRAS, 411, 1953

Queloz, D., Bouchy, F., Moutou, C., et al. 2009, A&A, 506, 303

Rauer, H., Queloz, D., Csizmadia, S., et al. 2009, A&A, 506, 281

Régulo, C., Almenara, J. M., Alonso, R., Deeg, H., & Roca Cortés, T. 2007, A&A, 467, 1345

Renner, S., Rauer, H., Erikson, A., et al. 2008, A&A, 492, 617

Southworth, J., Wheatley, P. J., & Sams, G. 2007, MNRAS, 379, L11

Surace, C., Alonso, R., Barge, P., et al. 2008, in Society of Photo-Optical Instrumentation Engineers (SPIE) Conference Series, Vol. 7019, Society of Photo-Optical Instrumentation Engineers (SPIE) Conference Series

Table 4. RV measurements for LRa01 planetary candidates.

BJD (days)	RV [km s^{-1}]	σ RV [km s^{-1}]	Instrument
LRa01 E1 0544			
2454766.69555	16.879	0.038	SOPHIE
2454767.64784	16.780	0.056	SOPHIE
LRa01 E1 0561			
2454515.34284	43.753	0.161	SOPHIE
2454526.33924	-8.432	0.132	SOPHIE
LRa01 E1 5015			
2455162.72198	62.831	0.246	HARPS
2455167.81154	92.556	0.251	HARPS
LRa01 E2 1123			
2454503.65300	-3.679	0.142	CORALIE
2454536.58722	-3.727	0.138	CORALIE
2454552.50781	-3.718	0.018	HARPS
2454555.53324	-3.686	0.020	HARPS
2454556.52061	-3.723	0.019	HARPS
2454557.52309	-3.729	0.017	HARPS
2454748.86821	-3.708	0.017	HARPS
2454762.82555	-3.673	0.015	HARPS
LRa01 E2 1145 = IRa01 E1 1873			
2454887.40723	25.201	0.073	SOPHIE
2454890.36710	71.572	0.069	SOPHIE
LRa01 E2 2249			
2454809.59849	36.297	0.017	SOPHIE
2454822.54316	60.556	0.011	SOPHIE
LRa01 E2 5084			
2455151.85444	81.812	0.497	HARPS
2455166.76997	8.308	0.385	HARPS
LRa01 E2 5184 = IRa01 E1 4108			
2454516.60149	99.250	0.024	HARPS
2454518.64495	99.220	0.031	HARPS
2454519.59227	99.321	0.032	HARPS
2455152.81296	99.261	0.021	HARPS
LRa01 E1 0286			
2454883.64831	118.833	0.124	SANDIFORD
2454885.78471	118.985	0.132	SANDIFORD
2455584.79281	121.705	0.112	SANDIFORD
2455591.77678	122.586	0.094	SANDIFORD
2455141.63827	115.928	0.012	SOPHIE
2455214.43238	118.123	0.014	SOPHIE
2455238.37453	120.656	0.021	SOPHIE
2455240.39734	120.891	0.015	SOPHIE
2455242.37050	121.088	0.011	SOPHIE
2455269.32548	124.209	0.010	SOPHIE
2455271.30759	124.406	0.008	SOPHIE
2455273.31278	124.586	0.015	SOPHIE
2455615.32719	124.981	0.009	SOPHIE
2455618.33486	125.277	0.009	SOPHIE
2455170.88184	-4.642	0.007	HIRES
2455171.14966	-4.638	0.007	HIRES
2455222.77727	-1.160	0.007	HIRES
2455223.92979	-1.052	0.007	HIRES
2455224.78564	-0.956	0.005	HIRES
2455225.06690	-0.922	0.005	HIRES
2455609.78808	4.419	0.010	HIRES
2455609.79556	4.421	0.007	HIRES
2455610.94623	4.530	0.008	HIRES
2455245.67304	121.487	0.003	HARPS

Table 4. Continued.

BJD (days)	RV [km s^{-1}]	σ RV [km s^{-1}]	Instrument
2455247.69007	121.710	0.013	HARPS
2455505.85621	115.387	0.005	HARPS
2455507.79110	115.391	0.004	HARPS
2455510.78882	115.451	0.006	HARPS
2455512.78152	115.504	0.005	HARPS
2455514.79798	115.575	0.004	HARPS
2455515.78588	115.607	0.005	HARPS
2455517.80895	115.668	0.003	HARPS
2455521.79614	115.842	0.009	HARPS
2455524.78741	115.995	0.004	HARPS
2455575.71323	120.612	0.007	HARPS
2455575.75009	120.618	0.004	HARPS
2455577.67357	120.845	0.006	HARPS
2455577.71019	120.844	0.006	HARPS
2455569.68872	119.876	0.025	FIES
2455581.46264	121.240	0.024	FIES
LRa01 E1 2101			
2455220.64433	0.907	0.012	HARPS
2455240.58607	0.909	0.028	HARPS
2455583.57129	0.928	0.013	HARPS
2455583.60336	0.921	0.017	HARPS
2455584.65380	0.903	0.020	HARPS
2455584.68555	0.955	0.018	HARPS
LRa01 E1 4667			
2455157.81799	26.205	0.078	HARPS
2455166.81523	26.121	0.056	HARPS
LRa01 E2 3156			
2455157.77092	82.084	0.033	HARPS
2455159.76521	82.118	0.035	HARPS
2455222.00327	0.013	0.017	HIRES
2455222.01408	-0.008	0.019	HIRES
2455222.73752	-0.001	0.019	HIRES
2455223.81145	0.000	0.019	HIRES
2455224.00538	0.000	0.017	HIRES
2455224.74151	-0.020	0.024	HIRES
2455610.92447	0.015	0.017	HIRES

Table 5. The *CoRoT* LRa01 planetary candidates: coordinates and transit parameters. The listed depth is relative to the combined total flux.

CoRoT ID	Win ID	α (J2000) [deg]	δ (J2000) [deg]	Epoch (HJD) [days]	Period [Days]	Depth %	Duration [Hours]
				Confirmed planets			
102764809	E1 1031	101.27723	0.81527	2454400.19885 ± 0.00020	4.037896 ± 0.000002	1.461	2.81
102708694	E2 0165	100.95606	-1.06303	2454398.07670 ± 0.00150	0.853585 ± 0.000024	0.034	1.25
102671819	E2 3459	100.76568	-1.29645	2454398.62707 ± 0.00036	2.828042 ± 0.000013	1.744	2.57
102725122	E2 5277	101.05245	-0.29913	2454399.02987 ± 0.00090	2.724740 ± 0.000140	0.449	4.76
				Settled cases: non planetary objects			
102714746	E1 0544	100.99094	0.73759	2454398.49627 ± 0.00001	2.75138 ± 0.00001	0.150	2.59
102597681	E1 0561	100.34489	-0.18307	2454426.95000 ± 0.00200	20.82000 ± 0.01000	0.700	3.60
102618931	E1 2890	100.47033	0.81683	2454399.29816 ± 0.00438	2.42955 ± 0.00026	0.286	1.70
102790970	E1 3666	101.42390	-0.14321	2454398.26940 ± 0.00300	1.55028 ± 0.00006	0.453	2.75
102777869	E1 5015	101.35044	0.46030	2454405.89953 ± 0.00006	13.68737 ± 0.00006	0.995	10.10
102692038	E1 4353	100.87058	0.24945	2454401.96117 ± 0.00001	5.23157 ± 0.00002	1.090	4.37
102615551	E2 1123	100.45001	-0.58771	2454400.84404 ± 0.00830	3.87707 ± 0.00004	1.800	1.08
102707895	E2 1145	100.95144	-0.96872	2454402.88326 ± 0.00630	5.78390 ± 0.00048	0.430	9.45
102658070	E2 1897	100.69371	-0.34008	2454402.33702 ± 0.00008	4.66957 ± 0.00008	2.800	3.65
102755811	E2 2249	101.22621	-0.76273	2454411.06010 ± 0.00490	27.92620 ± 0.00180	0.380	15.63
102723949	E2 2481	101.04563	-1.18701	2454426.74091 ± 0.00392	51.75900 ± 0.00590	1.200	0.80
102590741	E2 2694	100.29606	-0.97935	2454418.36090 ± 0.00670	30.39480 ± 0.00160	1.302	8.76
102590008	E2 4129	100.29088	-1.37087	2454398.24571 ± 0.00470	1.94250 ± 0.00010	0.175	2.02
102667981	E2 5084	100.74543	-1.03863	2454405.70210 ± 0.00450	9.91904 ± 0.00013	0.284	2.55
102779966	E2 5184	101.36197	-1.23596	2454403.17577 ± 0.00028	7.36827 ± 0.00028	0.410	2.68
102753331	E2 5747	101.21195	-0.71480	2454400.67866 ± 0.00740	19.75240 ± 0.00190	3.640	14.13
102755764	E2 3739	101.22575	-1.50861	2454426.27433 ± 0.00200	61.48000 ± 0.01000	2.930	6.97
102582529	E2 5756	100.23665	-0.43089	2454399.72057 ± 0.00029	15.84215 ± 0.00029	2.722	4.10
				Unsettled good planetary candidates			
102742060	E1 0286	101.14948	0.00790	2454398.70250 ± 0.01200	3.60207 ± 0.00005	0.031	1.80
102568803	E1 2101	100.13809	0.28304	2454464.06660 ± 0.00680	2.71839 ± 0.00051	0.079	1.00
102698887	E1 2240	100.90557	0.28097	2454463.10470 ± 0.00700	2.03187 ± 0.00047	0.094	2.10
102754163	E1 3216	101.21685	-0.06793	2454464.77560 ± 0.00740	3.11011 ± 0.00054	0.130	4.00
102634864	E1 3221	100.56930	0.83454	2454425.32970 ± 0.00210	32.32770 ± 0.00080	2.330	4.10
102782651	E1 4423	101.37645	0.99833	2454463.41470 ± 0.00930	1.86570 ± 0.00047	0.250	3.50
102617334	E1 4594	100.46082	-0.16461	2454398.58412 ± 0.01300	5.48907 ± 0.00091	0.270	6.62
102588881	E1 4667	100.28253	0.57086	2454409.36160 ± 0.00340	27.28810 ± 0.00120	1.520	2.64
102703155	E1 4719	100.92678	0.82986	2454463.08060 ± 0.00020	1.25939 ± 0.00020	0.099	0.97
102751316	E1 4820	101.20066	0.69970	2454399.51281 ± 0.00150	1.61152 ± 0.00003	0.463	1.43
102666452	E1 5320	100.73750	1.00772	2454463.64950 ± 0.00840	1.96423 ± 0.00480	0.140	3.30
102670085	E1 5536	100.75661	0.53083	2454398.54805 ± 0.00220	0.89910 ± 0.00010	0.270	1.54
102716818	E2 3156	101.00302	-0.43469	2454398.65000 ± 0.00500	1.47040 ± 0.00020	0.153	2.01
102765275	E2 3619	101.27973	-0.67173	2454431.97000 ± 0.01000	50.90780 ± 0.00300	5.960	7.00
102580137	E2 4519	100.21993	-0.45953	2454462.91720 ± 0.06500	2.37289 ± 0.00042	0.130	1.87
				Unsettled low priority planetary candidates			
102625386	E1 2970	100.51011	0.04896	2454400.16994 ± 0.00170	34.09600 ± 0.00400	0.622	5.90
102617210	E1 3617	100.46010	0.57616	2454463.42320 ± 0.00910	2.73050 ± 0.00074	0.640	3.86
102732757	E1 3674	101.09706	-0.06585	2454398.39349 ± 0.00370	1.96475 ± 0.00010	0.200	3.38
102626872	E1 4272	100.51949	1.04640	2454398.57854 ± 0.00200	1.87602 ± 0.00001	2.444	2.93
102620061	E1 4777	100.47743	0.45610	2454399.26041 ± 0.00170	3.34726 ± 0.00007	1.960	3.90
102630623	E1 4836	100.54263	0.47369	2454405.73688 ± 0.00220	36.76600 ± 0.00100	4.700	3.50
102595916	E1 5450	100.33219	0.07959	2454400.05000 ± 0.03200	4.11230 ± 0.00170	0.220	9.23
102729260	E2 2185	101.07759	-1.48648	2454399.74256 ± 0.00017	1.68885 ± 0.00017	0.240	3.57
102672065	E2 2597	100.76698	-1.41680	2454460.62310 ± 0.00070	8.89880 ± 0.00130	0.136	2.99
102757559	E2 2627	101.23591	-1.34969	2454463.26830 ± 0.01060	0.95085 ± 0.00021	0.083	4.80
102672700	E2 3157	100.77027	-0.36156	2454398.42115 ± 0.00300	1.86559 ± 0.00074	0.235	2.67
102587927	E2 4494	100.27591	-1.54206	2454399.68006 ± 0.01700	1.99270 ± 0.00040	0.130	2.81
102780627	E2 4910	101.36562	-0.58463	2454399.15242 ± 0.00021	2.38102 ± 0.00021	0.870	2.06
102604000	E2 5194	100.38392	-0.79700	2454398.07924 ± 0.00024	1.24861 ± 0.00024	0.684	2.79
				False alarms			
102613782	E1 2960	101.30976	-0.46050	2454451.73910 ± 0.01000	13.03130 ± 0.00330	0.170	9.50
102674894	E2 3389	100.78138	-1.27590	2454459.32040 ± 0.01000	7.03490 ± 0.00160	0.076	2.50
102577194	E2 3612	100.19875	-1.43906	2454423.34000 ± 0.11000	38.24000 ± 0.05000	0.340	8.56
				X-candidates			
102664130	E2 0928	100.72531	-0.28241	2454434.77350 ± 0.01000	49.90000 ± 0.10000	2.600	3.40
102613411	E2 5678	100.43715	-0.55653	2454412.56050 ± 0.00500	18.76330 ± 0.00050	4.330	8.00

Table 6. The *CoRoT* LRa01 planetary candidates: follow-up results.

Win ID	B [mag]	V [mag]	r' [mag]	i' [mag]	Candidate Nature[a]	Follow-up facilities Photometry	Spectroscopy	Comments
						Confirmed planets		
E1 1031	14.656	14.018	13.760	13.405	*CoRoT*-5b	IAC80	AAOmega, SOPHIE, HARPS	Rauer et al. (2009)
E2 0165	12.524	11.668	11.378	10.924	*CoRoT*-7b	CFHT, CST/FASTCAM, VLT/NACO, IAC80	AAOmega, FLAMES, CRIRES, HARPS, UVES	Léger et al. (2009); Queloz et al. (2009); Hatzes et al. (2010); Bruntt et al. (2010); Pont et al. (2011); Hatzes et al. (2011)
E2 3459	16.343	15.515	15.211	14.685	*CoRoT*-12b	IAC80	HARPS, HIRES	Gillon et al. (2010)
E2 5277	16.946	16.090	15.726	15.175	*CoRoT*-21b	IAC80	HARPS, HIRES	IAC80 confirms the transit is on target. F8 subgiant ($T_{\rm eff} \approx 6100$ K, $log\,g \approx 3.5$). HARPS and HIRES RVs data confirm a hot-Jupiter planet with $M_p \approx 2\,M_{Jup}$ (Pätzold et al. 2011).
						Settled cases: non planetary objects		
E1 0544	14.021	13.392	13.132	12.750	CEB	EulerCam, IAC80	AAOmega, SOPHIE	Classified as F7 V by AAOmega. The star is a fast rotator according to SOPHIE measurements and show no RV variation down to a precision of 50 m s^{-1}. EulerCam and IAC80 photometry reveals that a $\sim$ 4 magnitude fainter star located 9″ West of the main target contaminates the lightcurve with deep eclipses ($D \approx 20\,\%$).
E1 0561	12.417	12.000	11.826	11.589	SB3		AAOmega, SOPHIE, UVES	γ-Doradus variable star, classified as A7IV/V star by AAOmega. SOPHIE finds a low-contrast single peak CCF with a RV variation of about 52 km s^{-1}, in anti-phase with the *CoRoT* ephemeris. A single epoch UVES spectrum reveals a SB3 system.
E1 2890	17.189	15.732	15.121	14.215	CEB	IAC80		IAC80 observations find a contaminating eclipsing binary $\sim$ 12″ SE of target.
E1 3666	16.172	15.470	15.133	14.668	CEB	CFHT, IAC80		IAC80 and CHFT: contaminant star $\sim$ 8″ W of target shows 1.5 % variation consistent with transit signal.
E1 5015	17.167	16.168	15.743	15.087	SB1	ESA-OGS	HARPS	Transit duration of 10 hours indicates an eclipsing binary at photometric detection level. ESA-OGS observes the transit on target. 2 RV measurements with HARPS confirm a stellar binary system ($K = 16.5$ km s^{-1}).
E1 4353	16.369	15.775	15.521	15.145	CEB	EulerCam, IAC80		EulerCam finds that the transit-like signal is induced by a 5 % deep eclipse in a nearby contaminant star (*CoRoT* ID: 0102691690, V=16.7 mag). CEB scenario confirmed by IAC80.
E2 1123	15.934	14.622	13.983	13.185	Blend	IAC80, Wise	HARPS, CORALIE, UVES	Wise and IAC80 observe the transit on target. CORALIE and HARPS show a K5 V star with no detected RV variation at a level of about 50 m s^{-1}. UVES spectra reveal in the core of the Ca ɪɪ H & K lines 2 emission components whose RVs vary in phase at twice the transit period and with a maximum velocity difference of 67 km s^{-1}. Blend: suspected hierarchical triple system consisting of a K-dwarf orbited by two eclipsing M-type stars.
E2 1145	14.524	13.963	13.810	13.462	SB1		AAOmega, SOPHIE	Also known as IRa01 E1 1873. Classified as A9 IV/V by AAOmega. SOPHIE finds a RV variation with a semi-aplitude $K = 23.5$ km s^{-1} in anti-phase with the *CoRoT* ephemeris.
E2 1897	15.407	14.721	14.476	14.098	CEB	CFHT		Hints of a secondary eclipse are found in the lightcurve. Contamination by an eclipsing binary located $\sim$ 3″ NE from the main *CoRoT* target is found by CFHT photometry.
E2 2249	15.019	13.876	13.423	12.813	SB1		AAOmega, SOPHIE	K0 III/IV star based on AA0mega spectra. SOPHIE RV-measurements finds a RV semi-amplitude $K = 12$ km s^{-1} consistent with a binary system.
E2 2481	14.885	13.958	13.598	13.059	SB2		AAOmega, SOPHIE	Also a mono-transit candidate in IRa01, known as IRa01 E1 2046. AAOmega and SOPHIE identify this candidate as a binary system.
E2 2694	13.988	13.562	13.420	13.066	B3Ve star		AAOmega, SOPHIE, HARPS	SOPHIE and HARPS find no CCF, He ɪ absorption lines, and strong emission Balmer lines. AAOmega identifies the star as a B3 Ve star. If on target, the observed transit signal is caused by an eclipsing star.

Table 6. Continued.

Win ID	B [mag]	V [mag]	r' [mag]	i' [mag]	Candidate Nature[a]	Follow-up facilities Photometry	Spectroscopy	Comments
E2 4129	16.575	15.705	15.395	14.775	CEB	Eulercam, Wise		Wise observations are inconclusive. EulerCam reveals a 7 % drop in the flux of a contaminating star located ~ 4.5″ N-NE from the *CoRoT* target and responsible for the detected transit-like signal.
E2 5084	16.703	15.948	15.685	15.172	SB1		HARPS	HARPS reveals a SB1 system with a $K = 37.2$ km s^{-1} RV curve in anti-phase with the *CoRoT* ephemeris.
E2 5184	16.512	15.412	14.936	14.412	Blend	CFHT	HARPS	Also in IRa01 as IRa01 E1 4108. CFHT confirms the transit on-target. HARPS spectra yield $T_{\rm eff}$ =5000±100 K, $\log g$ =4.4±0.1 dex, $[M/H]$=0.07±0.06 dex, $v \sin i$ =1.5±0.5 km s^{-1}, and SpT=K0 V. HARPS CCF bisector variations identify candidate as a blend.
E2 5747	16.855	16.158	15.868	15.382	A-type star		HARPS	Also in IRa01 as IRa01 E1 4617. Transit duration and depth implies stellar companion. HARPS finds no CCF. Target star identified as a rapidly rotating A-type star. If on target, the observed transit signal is caused by an eclipsing star.
E2 3739	16.283	15.546	15.261	14.736	A-type star	EulerCam	HARPS	Also a mono-transit candidate in IRa01, known as IRa01 E1 4014. Transit depth, duration, and shape indicate grazing stellar eclipses. Transit observed by EulerCam 0.15 days after the predicted time, but still consistent with the transit event being on target. HARPS spectroscopy shows no CCF and a rapidly rotating A-type star. The observed transit signal is caused by an eclipsing star.
E2 5756	16.892	16.236	15.963	15.520	A-type star	IAC80	HARPS	Deep, shallow ingress/egress. Transit on target according to IAC80 observations. HARPS finds no CCF and a rapidly rotating A-type star. The observed transit signal is caused by an eclipsing star.

Unsettled good planetary candidates

Win ID	B [mag]	V [mag]	r' [mag]	i' [mag]	Candidate Nature[a]	Follow-up facilities Photometry	Spectroscopy	Comments
E1 0286	14.415	13.295	12.807	12.178	Unknown	CFHT, EulerCam	Sandiford, SOPHIE, HARPS, HIRES, FIES	Sandiford, HARPS, SOPHIE, HIRES, and FIES RV measurements show that the G8/9 IV primary star ($T_{\rm eff}$=5250±80 K, $\log g$=3.75±0.10 dex, $[M/H]$=-0.10±0.05 dex, $v \sin i$=3.0±1.0 km s^{-1}) belongs to a stellar binary system (P=337.52±0.20 days, e≈0.01, K=6.22±0.18 km s^{-1}, yielding M_2≈0.22 $M_\odot$ if M_1=1.10 $M_\odot$). No RV variation in phase with the *CoRoT* ephemeris is found in the RV residuals down to 5 m s^{-1}. CFHT and EulerCam photometric observations are not conclusive but might suggest a CEB scenario. The candidate is still under investigation.
E1 2101	15.257	14.153	13.509	12.907	Unknown	CFHT, MONET-North	HARPS	The lightcurve shows a spot-induced 2 % flux modulation with a period of ~11 days. The transit signal is only found in the *CoRoT* red channel because its depth is below the noise threshold in the green and blue channels. Combined measurements with CFHT and MONET-North exclude CEB. HARPS reveals K6 V star with $T_{\rm eff}$≈4250 K and $\log g$≈4.5 dex. Six HARPS RV measurements show no significant sinusoidal variation down to a precision of 18 m s^{-1}. The candidate is still under investigation.
E1 2240	15.859	15.221	14.914	14.475	Unknown			Asymmetric transit shape. Due to the low S/N ratio this is not conclusive to rule out the candidate.
E1 3216	16.470	15.694	15.331	14.856	Unknown			It shows shallow out-of-transit variations.
E1 3221	16.350	15.584	15.201	14.685	Unknown			V-shaped transit. Pulsations with periods of 0.78 and 8.75 days, typical of a giant, have been detected in the lightcurve, in disagreement with the A5 V classification reported in Exo-Dat.
E1 4423	17.528	16.224	15.569	14.805	Unknown			V-shaped transit. The lightcurve is strongly affected by instrumental effects (jumps).
E1 4594	18.182	16.657	15.993	14.692	Unknown	IAC80		The 6.6 hours transit duration suggests an evolved host star. IAC80 excludes nearby CEBs. Transit is concluded to be on target.

Table 6. Continued.

Win ID	B [mag]	V [mag]	r' [mag]	i' [mag]	Candidate Nature[a]	Follow-up facilities Photometry	Spectroscopy	Comments
E1 4667	16.845	16.084	15.575	15.029	Unknown	IAC80, Wise	HARPS	Wise photometric observations inconclusive due to bad weather. IAC80 photometry excludes contamination by background eclipsing binaries. Two HARPS spectra unveil a G0 V star and show a RV variation of 84 m s^{-1} which is comparable to the error bars ($\sim$70 m s^{-1}). The spectroscopic follow-up is still on-going.
E1 4719	16.577	15.881	15.520	15.049	Unknown	EulerCam		V-shaped and asymmetric transit shape. EulerCam might have missed the transit ground-based observations due to timing errors ($\pm$2 hours). Nevertheless, large photometric variations from nearby contaminant stars are probably not the cause for the observed transit event.
E1 4820	16.891	16.153	15.855	15.367	Unknown	ESA-OGS		Transit is on target according to OGS-ESA observations. Possible out of transit variations and depth differences between even/odd transits.
E1 5320	17.022	16.134	15.736	15.182	Unknown			Uncertain detection. The transit-like signal is only identified in the phase-folded lightcurve.
E1 5536	17.032	16.208	15.835	15.307	Unknown	CFHT		Although CFHT observed a 0.40 $\pm$ 0.25 % deep transit on target compatible with the *CoRoT* signal, some of the nearby background stars could not be excluded as possible contaminants. Observations are considered inconclusive.
E2 3156	17.211	15.757	15.127	14.271	Unknown	IAC80	HARPS, HIRES	The transit is only seen in the red *CoRoT* channel, is V-shaped, and has a long duration (2 hours) for a planetary object. According to IAC80 observations, background contaminants are probably excluded. There is a 20-30 % chance of missed transit due to timing errors. HARPS & HIRES find no RV variation down to a precision of 10 m s^{-1}. The candidate is still under investigation.
E2 3619	16.457	15.555	15.167	14.608	Unknown		AAOmega	Also in IRa01 as IRa01 E1 2060. G8 V star according to Exo-Dat. Classified as a G0 IV/V star by low-resolution AAOmega observations. *CoRoT* photometric data show multi-periodic variations with frequency spacing consistent with a giant. True spectral type unclear.
E2 4519	16.316	15.748	15.510	15.134	Unknown	EulerCam, IAC80		EulerCam and IAC80 observations show no photometric variations in any of the nearby stars. However, the transit may have been missed due to large (1.5 hours) timing errors. Likely on target.

Unsettled low priority planetary candidates

Win ID	B [mag]	V [mag]	r' [mag]	i' [mag]	Candidate Nature[a]	Follow-up facilities Photometry	Spectroscopy	Comments
E1 2970	15.057	14.487	14.263	13.837	Unknown			V-shaped transit signal detected only in the red channel. No significant detection in the blue and green channels. Hints of secondary eclipse in the red lightcurve. Suspected CEB.
E1 3617	16.432	15.618	15.219	14.722	Unknown			Several frequencies coherent with the transit period point to activities induced by a massive companion. Hints of secondary eclipses in the lightcurve. Suspected eclipsing binary.
E1 3674	15.785	15.324	15.146	14.842	Unknown			V-shaped transit, long duration, seen only in the red channel. No significant detection in the blue and green lightcurve. Suspected CEB.
E1 4272	16.750	15.868	15.506	14.889	Unknown	ESA-OGS		ESA-OGS confirms the transit signal to be on target. Out-of-transit variations detected in the lightcurve. Suspected eclipsing binary.
E1 4777	16.097	15.263	14.899	14.387	Unknown	IAC80		V-shaped transit, long duration, depth differences by more than 1 σ in the three color channels. No transit detected by IAC80, possibly due to underestimated transit timing error.
E1 4836	16.597	15.853	15.545	15.067	Unknown			V-shaped signal with significant (12 σ) depth difference between even and odd transits.
E1 5450	17.537	16.382	15.878	15.163	Unknown			Asymmetric transit shape. Duration too long to be consistent with a transiting planet.
E2 2185	15.830	15.078	14.772	14.299	Unknown			Also in IRa01 as IRa01 E1 1319. V-shaped long transit signal. Faint secondary eclipse at phase 0.5 and depth differences between even and odd transits suggest an eclipsing binary.

Table 6. Continued.

Win ID	B [mag]	V [mag]	r' [mag]	i' [mag]	Candidate Nature[a]	Follow-up facilities Photometry	Spectroscopy	Comments
E2 2597	15.286	14.165	13.753	12.980	Unknown		AAOmega, FLAMES	The signal is only present in the blue channel. No significant detection in the green and blue lightcurve. Classified as a G6 III/IV star by AAOmega. FLAMES yields $T_{\mathrm{eff}} = 4991 \pm 140$ K, $\log g = 3.24 \pm 0.30$ dex, $[M/H] = -0.29 \pm 0.15$ dex, and $v \sin i = 4.8 \pm 2.0$ km s^{-1}. Suspected CEB.
E2 2627	15.872	15.127	14.848	14.358	Unknown		AAOmega	V-shaped transit signal found only in the *CoRoT* blue channel. No significant detection in the red and green channels. Classified as F4 V by AAOmega. Suspected CEB.
E2 3157	15.990	14.858	14.351	13.715	Unknown			V-shaped signal found only in the red channel with significant (5σ) depth differences between even and odd transits. Suspected CEB.
E2 4494	17.225	16.069	15.561	14.795	Unknown			V-shaped transit, long duration.
E2 4910	16.240	15.357	14.977	14.447	Unknown	IAC80	AAOmega	Also in IRa01 as IRa01 E1 1531. Classified as a F7/8 V star according to AAOmega. IAC80 observes the transit on target. Secondary eclipses found in the lightcurve. Suspected eclipsing binary.
E2 5194	17.126	16.093	15.667	15.154	Unknown			Transit duration too long for a planetary companion.

False alarms

Win ID	B [mag]	V [mag]	r' [mag]	i' [mag]	Candidate Nature[a]	Follow-up facilities Photometry	Spectroscopy	Comments
E1 2960	15.144	14.400	14.061	13.625	Unknown			Transit-like signal detected only in the *CoRoT* red channel. Instrumental effects (jumps) in the lightcurve might mimic the transit-like signal.
E2 3389	16.948	15.649	15.087	14.127	Unknown			Instrumental effects (jumps) in the lightcurve might mimic the transit-like signal.
E2 3612	17.369	16.013	15.482	14.541	Unknown			Asymmetric transit shape. Instrumental effects (jumps) in the lightcurve might mimic the transit-like signal.

X-candidates

Win ID	B [mag]	V [mag]	r' [mag]	i' [mag]	Candidate Nature[a]	Follow-up facilities Photometry	Spectroscopy	Comments
E2 0928	16.035	15.618	15.476	15.220	Unknown			Too deep for a planetary candidate if spectral type is A5 IV (Exo-Dat). Needs spectral type confirmation.
E2 5678	16.505	15.909	15.617	15.257	Unknown			Too deep for a planetary candidate if spectral type is F5 V (Exo-Dat). Needs spectral type confirmation.

[a] The following abbreviations are used.
CEB: Contaminating eclipsing binaries
SB1: binary system with one component spectroscopically resolved
SB2: binary system with both components spectroscopically resolved
SB3: triple system with components spectroscopically resolved

Table 7. *CoRoT* eclipsing binary candidates found in LRa01.

CoRoT ID	Win ID	α (J2000) [deg]	δ (J2000) [deg]	V [mag]	Period [days]	σ Period [days]	Epoch [days] (HJD-2454000)	σ Epoch [days]	Duration [hours]	Depth [%]
102642448	E2 3931	100.61002	-1.03843	14.854	0.946162	0.000005	399.018180	0.000419	2.20	5.0
102671362	E2 3276	100.76310	-0.34620	15.369	0.861199	0.000014	398.875793	0.001268	3.90	14.1
102648472	E2 1645	100.64257	-0.57276	14.491	1.857077	0.000007	399.542170	0.000290	3.54	22.0
102645479	E1 2138	100.62651	0.96876	13.850	3.187703	0.000014	400.646979	0.000333	3.90	7.1
102681270	E2 1693	100.81449	-0.67801	14.674	2.986371	0.000012	400.722071	0.000354	3.90	30.9
102715227	E1 1535	100.99357	-0.17365	14.458	5.707336	0.000086	403.458115	0.001121	4.30	1.6
102669801	E1 0709	100.75499	0.24078	12.344	65.353042	0.001927	460.010802	0.001759	3.60	4.5
102648907	E2 3238	100.64484	-1.07534	14.526	18.778638	0.000225	412.732898	0.000695	2.50	4.2
102686781	E1 0596	100.84339	-0.10469	12.345	1.834789	0.000038	400.343875	0.001531	4.70	0.1
102683896	E2 3715	100.82835	-1.27826	14.612	32.036989	0.000387	415.994978	0.000706	4.40	8.3
102683427	E2 2833	100.82592	-0.55821	15.080	2.941566	0.000011	400.362048	0.000291	3.31	4.6
102689445	E1 2254	100.85702	0.11016	13.702	5.396659	0.000077	401.426186	0.000835	2.30	0.6
102692398	E2 3123	100.87232	-1.50637	15.161	1.426233	0.000013	399.271310	0.000706	5.90	40.0
102693162	E1 4520	100.87592	0.84680	15.215	6.287775	0.000019	402.949397	0.000227	3.90	8.7
102707160	E1 0819	100.94727	0.73391	14.875	6.692699	0.000065	403.705039	0.000767	4.20	1.1
102709642	E1 0902	100.96145	0.67965	12.399	14.307264	0.000061	408.969756	0.000284	6.00	5.7
102709715	E1 2274	100.96187	0.13496	13.540	6.403048	0.000031	404.172923	0.000332	7.50	27.5
102694654	E2 0798	100.88396	-0.92232	11.712	53.099729	0.005860	438.120036	0.004587	12.60	3.1
102697600	E2 1193	100.89890	-1.15852	14.059	3.450522	0.000018	400.436954	0.000392	4.50	1.4
102701940	E1 2387	100.92069	0.35024	15.204	1.442460	0.000009	399.064936	0.000494	3.00	10.0
102754263	E2 5118	101.21743	-1.05010	15.306	2.457281	0.000010	399.866496	0.000297	3.40	6.3
102756466	E2 3481	101.22988	-0.86304	15.478	16.770394	0.000260	411.880516	0.001077	10.30	5.7
102763847	E2 0588	101.27180	-1.35701	13.199	10.531476	0.000107	408.629758	0.000763	2.17	1.1
102732394	E2 4669	101.09488	-1.42804	14.965	1.573599	0.000004	399.322183	0.000203	2.35	7.1
102754051	E1 1586	101.21627	0.64393	14.899	1.166919	0.000023	399.544096	0.001478	3.01	0.3
102754203	E1 0117	101.21704	-0.07983	12.062	3.110191	0.000010	401.007376	0.000244	6.20	24.5
102782687	E1 4580	101.37667	-0.14502	15.133	2.035099	0.000009	399.763865	0.000368	3.50	3.8
102783117	E2 3914	101.37902	-0.66941	14.882	0.782120	0.000003	398.857435	0.000308	1.28	0.7
102785539	E2 1428	101.39257	-0.28442	14.412	8.387317	0.000083	404.242483	0.000722	5.02	5.1
102765275	E2 3619	101.27973	-0.67173	15.555	50.907326	0.004247	431.968060	0.003596	6.93	5.6
102770753	E1 2889	101.31062	0.24946	14.510	2.948118	0.000012	400.808644	0.000307	5.80	9.5
102778029	E1 0131	101.35131	0.25809	15.025	2.744178	0.000010	400.319192	0.000272	3.80	9.2
102738614	E2 3192	101.13036	-1.17246	14.452	7.768629	0.000031	403.825388	0.000293	4.40	14.3
102738809	E1 0830	101.13139	0.83213	12.446	2.035701	0.000005	400.375297	0.000171	3.70	21.2
102715978	E2 0655	100.99809	-1.49286	13.130	2.977287	0.000006	401.151276	0.000157	2.75	7.5
102717012	E1 1152	101.00412	0.14640	14.245	3.541248	0.000049	403.666723	0.001027	4.80	0.4
102726405	E2 0081	101.06131	-1.37603	12.759	2.542021	0.000008	399.886189	0.000255	7.70	15.4
102749942	E2 2040	101.19331	-1.25734	15.157	2.766452	0.000007	400.341204	0.000202	3.70	9.0
102752091	E1 0921	101.20481	0.35313	13.788	24.110928	0.000154	415.798900	0.000466	4.90	7.5
102752663	E1 0256	101.20823	0.01468	12.998	1.428129	0.000005	399.104904	0.000265	2.19	16.8
102740965	E2 0133	101.14347	-1.31865	14.360	1.427733	0.000004	399.584562	0.000216	4.02	13.6
102745334	E1 1045	101.16745	0.36468	12.851	3.329436	0.000008	400.776142	0.000190	5.10	5.9

Table 7. Continued.

CoRoT ID	Win ID	α (J2000) [deg]	δ (J2000) [deg]	V [mag]	Period [days]	σ Period [days]	Epoch [days] (HJD-2454000)	σ Epoch [days]	Duration [hours]	Depth [%]
102748636	E1 2309	101.18618	0.04554	15.153	1.682770	0.000006	399.777365	0.000288	1.93	4.2
102585693	E2 3406	100.25972	-0.38510	14.488	1.944186	0.000006	399.638928	0.000263	3.70	14.1
102579996	E2 2038	100.21891	-0.37308	14.770	2.421712	0.000007	400.062064	0.000230	4.90	28.1
102578195	E1 5333	100.20590	0.33968	15.681	1.017308	0.000003	399.295603	0.000204	2.10	11.4
102584675	E1 2146	100.25228	-0.06009	15.192	35.185560	0.002234	420.942262	0.004179	5.50	1.6
102584601	E2 0427	100.25183	-0.36270	12.958	2.212568	0.000005	400.328584	0.000171	3.00	2.5
102577917	E2 3194	100.20377	-0.65305	14.705	28.624755	0.000251	414.036052	0.000626	4.00	13.1
102588918	E1 0891	100.28279	0.96940	13.977	1.105403	0.000007	399.357583	0.000534	3.90	0.8
102786821	E2 1665	101.39994	-1.32339	14.710	1.918821	0.000021	400.304029	0.000830	2.95	0.9
102663890	E1 5182	100.72404	0.33139	15.387	0.982197	0.000021	399.251874	0.001483	1.71	0.1
102638391	E1 3900	100.58806	1.07756	15.021	3.594890	0.000044	402.097165	0.000846	12.40	47.1
102619084	E2 5138	100.47146	-1.50041	15.500	2.321641	0.000008	400.576933	0.000273	5.50	15.3
102617617	E1 3453	100.46259	-0.17071	14.847	5.491371	0.000036	404.070019	0.000455	6.50	11.2
102627177	E2 3716	100.52137	-0.70129	15.443	7.134999	0.000049	404.650410	0.000501	3.40	2.3
102621867	E1 2848	100.48846	0.85040	15.471	2.330957	0.000011	400.113175	0.000386	3.55	9.2
102608434	E1 0795	100.40904	0.67243	13.896	2.123260	0.000009	400.347289	0.000310	2.40	6.3
102614893	E2 2631	100.44562	-0.60833	14.990	4.955753	0.000012	402.266779	0.000172	4.30	27.9
102598640	E1 4306	100.35083	0.54177	15.558	1.611417	0.000006	399.767013	0.000293	3.90	1.8
102609164	E1 3191	100.41325	0.28558	14.671	0.907682	0.000007	398.882958	0.000629	3.90	58.0
102573289	E1 1225	100.17053	0.08003	14.653	2.111770	0.000007	399.843150	0.000255	4.70	2.9
102795835	E2 2759	101.45509	-0.57540	15.167	1.396369	0.000024	399.380195	0.001241	3.61	0.4
102790592	E1 1968	101.42181	-0.13084	14.961	1.312664	0.000012	399.210125	0.000718	2.17	0.4
102790542	E1 4534	101.42156	-0.08875	16.035	2.636270	0.000037	400.973137	0.000756	2.44	0.6
102786471	E2 0108	101.39791	-0.36788	14.719	1.064925	0.000003	399.479925	0.000193	3.28	53.8
102746008	E1 2243	101.17122	0.12372	15.537	1.161180	0.000025	399.272108	0.001357	2.44	0.2
102735868	E2 4308	101.11474	-1.33074	15.249	1.647077	0.000011	399.918786	0.000483	3.77	8.0
102726103	E2 1431	101.05957	-1.22901	14.541	3.814844	0.000057	401.213655	0.001104	1.80	0.5
102713211	E1 0268	100.98200	1.03019	12.298	1.721961	0.000011	399.524813	0.000491	3.21	5.7
102697826	E2 1309	100.90022	-1.11005	14.686	3.773479	0.000572	402.383534	0.010650	4.93	0.1
102692686	E1 2646	100.87365	1.08987	14.314	10.225294	0.000817	408.106382	0.005185	4.91	1.8
102682858	E1 2276	100.82297	-0.16174	14.925	4.252979	0.000138	401.328311	0.002237	2.97	0.3
102677981	E2 0711	100.79730	-1.35050	13.491	2.196415	0.000006	399.605245	0.000192	2.12	1.8
102644596	E1 2373	100.62169	1.04022	15.228	0.826135	0.000013	398.875267	0.001219	2.80	0.4
102634660	E2 2797	100.56807	-1.18100	13.896	0.850421	0.000014	399.211761	0.001280	4.30	13.5
102609031	E2 0149	100.41252	-0.33838	12.637	2.405687	0.000663	399.751818	0.020360	4.84	0.03
102595682	E2 1885	100.33055	-0.66220	14.729	11.555735	0.000475	409.782628	0.002373	4.47	0.6
102594380	E1 0221	100.32172	0.12202	12.003	4.265298	0.000499	401.622961	0.006218	5.10	0.03
102594134	E1 0833	100.31997	0.44688	13.839	0.789493	0.000008	399.065729	0.000771	2.99	0.3
102582070	E2 2085	100.23336	-0.36338	14.790	1.365732	0.000031	399.112761	0.001391	1.47	0.1
102779171	E2 0741	101.35745	-1.06390	13.443	11.340428	0.000327	404.558176	0.001922	6.03	0.7
102776522	E1 0957	101.34317	0.52667	14.043	1.885600	0.000201	400.230930	0.007385	3.65	0.3
102601239	E2 1907	100.36812	-0.67659	16.266	4.653853	0.000052	401.876710	0.000843	2.70	1.9
102717803	E2 3220	101.00886	-0.54199	14.844	1.933542	0.000031	400.236831	0.001238	3.37	0.5

Table 7. Continued.

CoRoT ID	Win ID	α (J2000) [deg]	δ (J2000) [deg]	V [mag]	Period [days]	σ Period [days]	Epoch [days] (HJD-2454000)	σ Epoch [days]	Duration [hours]	Depth [%]
102580849	E2 1202	100.22476	-0.60653	14.188	9.122674	0.000263	403.789057	0.002039	4.13	0.6
102633553	E1 3270	100.56155	0.04144	15.557	2.946338	0.000138	402.020597	0.003524	4.75	0.5
102576377	E2 0405	100.19290	-0.65223	13.522	3.288979	0.000042	401.105280	0.000950	2.63	0.5
102762822	E2 4634	101.26607	-1.51980	15.461	4.771849	0.000531	401.975713	0.007829	1.10	0.2
102636305	E1 1925	100.57696	0.00786	15.017	1.950456	0.000187	398.528920	0.006352	1.00	0.1
102714427	E1 1589	100.98910	0.35167	12.398	1.889818	0.000013	399.841005	0.000573	2.38	0.7
102779728	E1 1058	101.36067	-0.01903	14.182	0.966148	0.000027	399.190879	0.001979	1.60	2.0
102757626	E2 3231	101.23632	-1.23750	14.698	1.205370	0.000006	399.286274	0.000355	4.00	8.3
102705738	E2 3982	100.93946	-1.47825	15.686	0.875843	0.000007	398.814761	0.000616	2.13	0.8
102694263	E2 1439	100.88186	-0.71382	14.371	1.283256	0.000020	399.300581	0.001177	3.45	0.3
102645479	E1 2138	100.62651	0.96876	13.850	3.187703	0.000014	400.646979	0.000333	3.90	7.1
102641748	E1 0144	100.60639	0.63014	11.518	3.376244	0.000066	400.931359	0.001429	10.50	0.3
102641637	E1 5485	100.60583	0.55097	15.133	1.208779	0.000005	399.542439	0.000336	3.44	9.7
102619157	E2 1217	100.47197	-0.93956	13.741	1.960673	0.000005	400.272383	0.000203	2.10	2.7
102617194	E2 2385	100.46001	-1.24594	14.367	1.027648	0.000006	399.287436	0.000448	3.27	5.6
102614969	E1 0606	100.44614	0.53275	14.498	4.312780	0.000103	402.527150	0.001855	4.78	0.4
102607016	E1 2015	100.40079	-0.13671	14.728	0.946957	0.000006	399.015273	0.000516	2.70	4.1
102602947	E1 2450	100.37799	0.32808	15.323	2.132231	0.000010	399.833390	0.000377	2.68	1.6
102597871	E1 0591	100.34619	-0.10124	13.405	1.885878	0.000010	399.527123	0.000351	5.70	6.7
102596999	E2 1564	100.33984	-1.14952	14.376	0.743465	0.000019	398.865269	0.001967	3.60	19.0
102578549	E2 3158	100.20852	-0.61047	15.451	4.804970	0.000114	402.233387	0.001816	3.85	0.6
102643106	E2 0858	100.61330	-1.56419	13.603	1.616385	0.000009	399.775376	0.000434	2.49	1.9
102708522	E2 2581	100.95508	-1.24974	15.241	49.951670	0.001424	423.628583	0.001964	31.20	43.0
102708916	E2 2754	100.95732	-0.79757	13.969	6.189113	0.000034	403.883384	0.000391	5.62	13.3
102673160	E2 0452	100.77262	-0.57780	12.941	28.919025	0.000365	419.219923	0.000620	8.89	23.7
102679883	E1 2999	100.80728	0.40780	14.341	13.124338	0.000111	410.739834	0.000557	6.00	21.5
102698865	E2 0805	100.90544	-1.10792	13.414	3.773426	0.000030	402.387915	0.000579	6.90	24.0
102768841	E2 0547	101.29985	-1.19510	12.268	54.144213	0.003494	445.717633	0.004336	24.70	4.1
102771617	E1 3793	101.31557	0.35420	14.690	3.512354	0.000015	401.838753	0.000336	3.92	10.2
102785122	E2 5530	101.39016	-0.43924	14.112	14.231446	0.000101	412.429126	0.000505	6.16	9.9
102709152	E2 1636	100.95867	-1.54322	13.939	18.830609	0.001128	417.590398	0.002241	8.46	5.0
102734453	E2 1413	101.10663	-0.67484	14.467	8.371161	0.000072	407.042490	0.000554	6.45	13.5
102753648	E1 2396	101.21385	0.23205	13.913	21.707185	0.000251	414.419258	0.000705	3.16	14.7
102600548	E2 1265	100.36368	-1.26725	12.640	20.784417	0.000163	416.879862	0.000492	5.05	3.2
102604360	E2 1584	100.38603	-0.71627	14.495	9.696161	0.000058	405.080551	0.000442	5.27	16.9
102610389	E1 1952	100.41996	0.13334	14.975	12.241350	0.000093	400.084212	0.000537	4.07	11.7
102574112	E1 2277	100.17657	0.18288	15.197	3.377023	0.000017	401.030513	0.000356	3.51	12.7
102634420	E1 3781	100.56688	-0.18196	14.457	8.749810	0.000090	407.208618	0.000717	10.20	11.1
102647241	E2 0669	100.63591	-0.59356	12.007	39.796209	0.022271	419.634256	0.031942	31.00	5.0
102672710	E2 1731	100.77033	-0.76676	14.627	2.571543	0.000005	399.152690	0.000144	3.80	12.6
102618087	E2 1627	100.46524	-0.62782	13.009	3.143964	0.000006	398.685790	0.000137	7.70	26.6
102629072	E1 1409	100.53311	0.72926	14.569	7.837330	0.000044	403.815125	0.000389	6.50	6.3
102631435	E2 0876	100.54771	-1.27862	13.785	1.300104	0.000004	399.360869	0.000243	3.45	6.7

Table 7. Continued.

CoRoT ID	Win ID	α (J2000) [deg]	δ (J2000) [deg]	V [mag]	Period [days]	σ Period [days]	Epoch [days] (HJD-2454000)	σ Epoch [days]	Duration [hours]	Depth [%]
102713490	E1 4893	100.98373	0.81960	15.974	0.777131	0.000003	399.003553	0.000353	2.42	1.6
102733791	E1 3958	101.10301	0.25379	15.669	2.282416	0.000007	399.889715	0.000211	4.30	18.2
102773381	E1 5455	101.32541	1.00587	16.112	4.378467	0.000015	401.183259	0.000258	6.10	9.9
102674581	E2 5417	100.77962	-0.63989	15.876	70.894514	0.001447	453.241151	0.000767	4.13	11.6
102680756	E2 4200	100.81173	-0.39709	15.649	2.007137	0.000026	399.593647	0.001009	2.25	0.4
102694531	E1 5366	100.88332	0.29719	16.171	2.876634	0.000007	400.476568	0.000190	3.02	13.0
102787432	E1 5106	101.40336	1.04653	16.297	2.976988	0.000006	401.107130	0.000155	3.10	31.8
102792220	E1 4365	101.43104	0.35033	15.942	4.979622	0.000015	402.901069	0.000224	3.57	7.0
102734729	E1 5263	101.10819	0.49287	16.094	1.844295	0.000007	399.563746	0.000284	2.70	5.7
102739450	E2 3753	101.13502	-0.64769	15.620	2.072752	0.000033	400.438180	0.001295	2.96	0.4
102770690	E1 4585	101.31025	-0.14371	16.260	9.181396	0.000106	404.659443	0.000820	2.96	5.0
102594502	E1 3756	100.32252	0.73792	15.787	4.553217	0.000014	402.950194	0.000229	4.90	20.2
102600961	E2 3166	100.36651	-1.38743	15.861	2.615209	0.000010	400.225430	0.000311	3.60	6.2
102584027	E2 4570	100.24757	-0.76872	15.983	0.834312	0.000003	398.893914	0.000303	2.60	39.2
102588594	E1 3870	100.28060	0.94613	15.900	3.253552	0.000060	400.413761	0.001258	3.05	0.4
102627368	E2 3560	100.52254	-0.47978	15.591	4.563484	0.000037	401.379037	0.000613	4.12	1.1
102636324	E2 5310	100.57707	-1.52046	16.215	0.722200	0.000004	399.017935	0.000407	2.80	2.0
102611651	E1 4413	100.42711	0.93444	16.124	2.698682	0.000009	400.737339	0.000269	3.90	7.8
102667674	E2 3920	100.74380	-1.33441	15.624	1.377211	0.000003	398.428467	0.000175	3.40	12.0
102620895	E1 4525	100.48263	0.29622	15.858	1.744066	0.000011	399.429713	0.000474	3.36	3.5
102577212	E1 5474	100.19888	0.45315	16.328	2.350945	0.000010	400.184694	0.000352	2.42	2.2
102786829	E2 5272	101.39999	-0.62990	16.211	0.750877	0.000009	399.062756	0.000931	2.84	0.3
102738837	E1 0169	101.13160	0.39014	15.622	0.846455	0.000008	399.055066	0.000653	2.99	1.4
102738514	E2 5556	101.12969	-0.95544	16.193	1.150231	0.000007	399.570411	0.000472	3.29	2.9
102726103	E2 1431	101.05957	-1.22901	14.541	3.814844	0.000057	401.213655	0.001104	1.80	0.5
102700859	E2 4360	100.91538	-0.34657	15.730	92.054080	0.003335	420.928803	0.002557	10.21	3.5
102689472	E2 5564	100.85715	-1.32048	16.614	39.156658	0.003177	421.735630	0.003093	6.96	1.2
102672357	E1 3833	100.76848	0.38261	15.721	1.460559	0.000015	399.312002	0.000800	3.61	0.6
102647789	E2 5778	100.63895	-0.50480	16.127	1.891158	0.000010	399.522050	0.000393	4.93	7.3
102584786	E2 0980	100.25306	-0.77015	12.911	0.834130	0.000018	399.331667	0.001617	2.99	0.0
102577141	E1 5717	100.19831	0.60752	16.395	1.305379	0.000021	399.732210	0.001349	2.88	0.3
102733319	E1 1362	101.10039	0.91484	14.427	3.712853	0.000225	399.998256	0.004245	2.08	0.2
102724976	E1 3903	101.05169	0.50670	15.608	1.960502	0.000009	399.382255	0.000362	1.96	3.7
102680399	E1 4038	100.80982	0.28473	15.602	1.155279	0.000021	399.037300	0.001315	2.44	0.2
102578884	E1 4407	100.21085	0.31608	15.957	12.594412	0.000505	410.657071	0.002716	4.11	0.8
102763199	E2 4333	101.26822	-0.27984	15.891	1.357588	0.000010	399.445576	0.000567	2.04	0.7
102756903	E2 4873	101.23213	-1.44495	15.905	0.979106	0.000004	398.567653	0.000323	2.13	2.7
102656104	E2 2329	100.68334	-0.42648	15.914	2.850244	0.000016	399.986355	0.000503	3.61	7.2
102745492	E2 1533	101.16840	-1.12118	16.271	3.604739	0.000019	398.493123	0.000377	3.20	4.6
102605747	E1 3848	100.39355	0.27810	15.779	1.765928	0.000019	400.017956	0.000773	3.79	0.8
102671472	E1 3766	100.76369	0.80438	15.610	8.753344	0.000136	404.681792	0.001032	6.55	3.9
102747001	E1 4179	101.17670	1.03283	15.837	11.779580	0.000781	399.723928	0.004092	4.70	0.4
102701904	E2 4508	100.92051	-0.88977	15.525	21.069530	0.002498	405.917129	0.007172	5.06	0.4

Table 7. Continued.

CoRoT ID	Win ID	α (J2000) [deg]	δ (J2000) [deg]	V [mag]	Period [days]	σ Period [days]	Epoch [days] (HJD-2454000)	σ Epoch [days]	Duration [hours]	Depth [%]
102696330	E2 0740	100.89250	-1.50445	13.082	1.425823	0.000187	398.591040	0.011157	6.20	0.02
102673717	E2 5640	100.77555	-1.02062	16.064	1.392683	0.000037	399.592129	0.002165	3.00	0.3
102651872	E2 3754	100.66057	-1.25510	15.756	1.432223	0.000039	398.838574	0.001643	4.20	0.2
102666497	E2 5134	100.73776	-1.45424	15.826	2.686807	0.000012	399.850990	0.000312	3.15	3.1
102661821	E2 5332	100.71314	-1.52446	16.120	6.251454	0.000050	404.781743	0.000615	4.20	6.8
102659695	E1 5762	100.70192	0.63444	15.853	13.410774	0.000158	409.518970	0.000826	5.30	5.0
102715122	E1 0627	100.99293	-0.11182	16.156	35.012757	0.000566	421.195976	0.000101	5.50	8.0
102669560	E1 5150	100.75378	0.42345	16.271	31.184604	0.000504	411.458970	0.001197	6.20	10.0
102752408	E2 5357	101.20673	-1.12243	16.128	21.267535	0.001093	417.054930	0.002680	3.92	0.9
102631623	E1 4645	100.54878	0.58558	16.088	12.189919	0.000213	402.352840	0.001133	11.60	15.8
102613810	E2 4235	100.43932	-1.28874	15.539	1.688546	0.000003	399.682340	0.000145	5.00	27.7
102642253	E1 1574	100.60898	0.42241	11.445	0.5504108	0.000005	397.938360	0.000700	7.20	17.0
102642253	E1 1574	100.60898	0.42241	11.445	4.3408	0.000100	398.860000	0.010000	3.20	1.3
102745707	E1 0622	101.16961	0.31719	13.570	0.288536	0.000001	397.749020	0.000280	1.60	49.0
					Mono-transits					
102647266	E1 2765	100.63604	0.96943	15.339	-	-	465.434000	0.010000	5.00	8.3
102709133	E1 4785	100.95856	0.07081	16.576	-	-	419.798000	0.010000	7.50	9.7
102574444	E2 1113	100.17892	-0.67400	14.812	-	-	422.342000	0.010000	4.60	5.4
102582649	E2 2368	100.23747	-0.63648	15.673	-	-	510.992000	0.010000	5.90	17.8
102586624	E2 2744	100.26644	-0.38891	15.767	-	-	473.174000	0.010000	6.30	15.8

[1] Rheinisches Institut für Umweltforschung, Abteilung Planetenforschung, an der Universität zu Köln, Aachener Strasse 209, 50931, Germany
e-mail: lcarone@uni-koeln.de

[2] Research and Scientific Support Department, ESTEC/ESA, PO Box 299, 2200 AG Noordwijk, The Netherlands
e-mail: davide.gandolfi@esa.int

[3] Thüringer Landessternwarte, Sternwarte 5, Tautenburg, D-07778 Tautenburg, Germany

[4] Institute of Planetary Research, German Aerospace Center, Rutherfordstrasse 2, 12489 Berlin, Germany

[5] LUTH, Observatoire de Paris, CNRS, Université Paris Diderot; 5 place Jules Janssen, 92195 Meudon, France

[6] Instituto de Astrofísica de Canarias, E-38205 La Laguna, Tenerife, Spain

[7] Departamento de Astrofísica, Universidad de La Laguna, 38206 La Laguna, Tenerife, Spain

[8] Space Research Institute, Austrian Academy of Science, Schmiedlstr. 6, A-8042 Graz, Austria

[9] Oxford Astrophyiscs, Denys Wilkinson Building, Keble Road, Oxford OX1 3RH

[10] Observatoire de l'Université de Genève, 51 chemin des Maillettes, 1290 Sauverny, Switzerland

[11] School of Physics, University of Exeter, Stocker Road, Exeter EX4 4QL, United Kingdom

[12] Laboratoire d'Astrophysique de Marseille, CNRS & University of Provence, 38 rue Frédéric Joliot-Curie, 13388 Marseille cedex 13, France

[13] LESIA, Observatoire de Paris, Place Jules Janssen, 92195 Meudon cedex, France

[14] Institut d'Astrophysique Spatiale, Université Paris XI, F-91405 Orsay, France

[15] Institut d'Astrophysique de Paris, UMR7095 CNRS, Université Pierre & Marie Curie, 98bis boulevard Arago, 75014 Paris, France

[16] Observatoire de Haute Provence, 04670 Saint Michel l'Observatoire, France

[17] McDonald Observatory, University of Texas at Austin, Austin, TX 78712, USA

[18] Institut für Astrophysik, Georg-August-Universität, Friedrich-Hund-Platz 1, D-37077 Göttingen, Germany

[19] University of Vienna, Institute of Astronomy, Türkenschanzstrasse 17, A-1180 Vienna, Austria

[20] IAG, University of São Paulo, Brasil

[21] Université de Nice-Sophia Antipolis, CNRS UMR 6202, Observatoire de la Côte d'Azur, BP 4229, 06304 Nice Cedex 4, France

[22] University of Liège, Allée du 6 août 17, Sart Tilman, Liège 1, Belgium

[23] European Southern Observatory, Alonso de Córdova 3107, Casilla 19001, Santiago de Chile, Chile

[24] School of Physics and Astronomy, Raymond and Beverly Sackler Faculty of Exact Sciences, Tel Aviv University, Tel Aviv, Israel

[25] Departamento de Astronomía y Astrofísica, Pontificia Universidad Católica de Chile, Casilla 306, Santiago 22, Chile

[26] Center for Astronomy and Astrophysics, TU Berlin, Hardenbergstr. 36, 10623 Berlin, Germany

[27] Laboratoire d'Astronomie de Lille, Université de Lille 1, 1 impasse de l'Observatoire, 59000 Lille, France

[28] Institut de Mécanique Céleste et de Calcul des Ephémérides, UMR 8028 du CNRS, 77 avenue Denfert-Rochereau, 75014 Paris, France

[29] Observatório Nacional, Rio de Janeiro, Brazil

[30] Las Cumbres Observatory Global Telescope Network, Inc., 6740 Cortona Drive, Suite 102, Santa Barbara, California 93117, USA